U. S. Department of
Transportation
**Federal Railroad
Administration**

# Passenger Rail Two-Car Impact Test Volume I: Overview and Selected Results

Office of Research
and Development
Washington, D.C. 20590

## Rail Passenger Equipment Collision Tests


**DOT/FRA/ORD-01/22.I**

**Final Report
January 2002**

**This document is available to the public through the National Technical Information Service, Springfield, VA 22161
This document is also available on the FRA web site at www.fra.dot.gov**

# REPORT DOCUMENTATION PAGE

*Form Approved*
*OMB No. 0704-0188*



| 1. AGENCY USE ONLY (Leave blank) | 2. REPORT DATE | 3. REPORT TYPE AND DATES COVERED |
|---|---|---|
| | January 2002 | Final Report<br>April 2000 – November 2000 |

4. TITLE AND SUBTITLE
Passenger Rail Two-Car Impact Test Volume I: Overview and Selected Results

5. FUNDING NUMBERS
RR128/R1001

6. AUTHOR(S)
David Tyrell, Kristine Severson, John Zolock, A. Benjamin Perlman

7. PERFORMING ORGANIZATION NAME(S) AND ADDRESS(ES)
U.S. Department of Transportation
Research and Special Programs Administration
John A. Volpe National Transportation Systems Center
55 Broadway
Cambridge, MA 02142-0193

8. PERFORMING ORGANIZATION REPORT NUMBER
DOT-VNTSC-FRA-01-08.1

9. SPONSORING/MONITORING AGENCY NAME(S) AND ADDRESS(ES)
U.S. Department of Transportation
Federal Railroad Administration
Office of Research and Development
1120 Vermont Avenue, NW - Mail Stop 20
Washington, DC 20590

10. SPONSORING/MONITORING AGENCY REPORT NUMBER
DOT/FRA/ORD-01/22.I

11. SUPPLEMENTARY NOTES

12a. DISTRIBUTION/AVAILABILITY STATEMENT
This document is available to the public through the National Technical Information Service, Springfield VA 22161
This document is also available on the FRA web site at www.fra.dot.gov.

12b. DISTRIBUTION CODE

13. ABSTRACT (Maximum 200 words)
A full-scale, two-car impact test was conducted on April 4, 2000. Two coupled rail passenger cars impacted a fixed barrier at 26 mph. The cars were instrumented with strain gauges, accelerometers, and string potentiometers to measure the deformation of critical structural elements, the longitudinal, vertical, and lateral car body accelerations, and the displacements of the truck suspensions. Instrumented crash-test dummies were also tested in several seat configurations, with and without lap and shoulder belts.

The objectives of the two-car test were to measure the gross motions of the car, to measure the force/crush characteristic, to observe the car-to-car interaction, to observe failure modes of the major structural components, and to evaluate selected occupant protection strategies. The measurements taken during the test were used to refine and validate existing computer models of conventional passenger rail vehicles. This test was the second in a series of collision tests designed to characterize the collision behavior of rail vehicles.

The two-car test resulted in approximately 6 feet of deformation at the impacting end of the lead vehicle, and a few inches of deformation at the coupler. The cars remained coupled, but buckled in a saw-tooth mode, with a 15-inch lateral displacement between the cars after the test.

The test data from the two-car test compared favorably with data from the single-car test, and with analysis results developed with a lumped-mass computer model. The model is described in detail. The methods of filtering and interpreting the test data are also included.

14. SUBJECT TERMS
Transportation, safety, crashworthiness, occupant protection, rail vehicles

15. NUMBER OF PAGES
50

16. PRICE CODE

| 17. SECURITY CLASSIFICATION OF REPORT | 18. SECURITY CLASSIFICATION OF THIS PAGE | 19. SECURITY CLASSIFICATION OF ABSTRACT | 20. LIMITATION OF ABSTRACT |
|---|---|---|---|
| Unclassified | Unclassified | Unclassified | |

# PREFACE

This work was performed as part of the Equipment Safety Research Program sponsored by the Office of Research and Development of the Federal Railroad Administration. The authors would like to thank Tom Tsai, Program Manager, and Claire Orth, Division Chief, Equipment and Operating Practices Research Division, Office of Research and Development, Federal Railroad Administration, for their support.

Gunars Spons, Federal Railroad Administration Resident Engineer at the Transportation Technology Center, Inc., directed and coordinated the activities of all the parties involved in the test. Barrie Brickle, Senior Engineer, Transportation Technology Center, Inc., implemented the equipment-related portions of the test. Caroline Van Ingen-Dunn, Senior Engineer, Simula Technologies, Inc., implemented the occupant-protection tests.

The authors would like to thank Edward Murphy, Chief Mechanical Officer, Southeastern Pennsylvania Transportation Authority, for arranging the donation of the cars in the test effort, Doug Karan of Amtrak for arranging the donation of the intercity passenger seats, and Gordon Campbell, Senior Engineer, LDK Engineering, Inc., for securing a copy of the Pioneer car structural drawings from Bombardier, Inc. Thomas Peacock of the American Public Transportation Association was exceptionally effective in his efforts to coordinate the test with members of the passenger-rail transportation industry.

The authors would also like to thank Roy Allen, President, Transportation Technology Center, Inc., and his staff for hosting the guests who came to view the test, for arranging a tour of the facilities at the Transportation Technology Center for those guests, and for their support in working with the media.

The authors would like to acknowledge the assistance of the United States Department of Transportation's National Highway Transportation Safety Administration, which provided six test dummies, and the US DOT's Federal Aviation Administration, which provided four load cells.

## METRIC/ENGLISH CONVERSION FACTORS

| ENGLISH TO METRIC | METRIC TO ENGLISH |
|---|---|
| **LENGTH (APPROXIMATE)** | **LENGTH (APPROXIMATE)** |
| 1 inch (in) = 2.5 centimeters (cm) | 1 millimeter (mm) = 0.04 inch (in) |
| 1 foot (ft) = 30 centimeters (cm) | 1 centimeter (cm) = 0.4 inch (in) |
| 1 yard (yd) = 0.9 meter (m) | 1 meter (m) = 3.3 feet (ft) |
| 1 mile (mi) = 1.6 kilometers (km) | 1 meter (m) = 1.1 yards (yd) |
| | 1 kilometer (km) = 0.6 mile (mi) |
| **AREA (APPROXIMATE)** | **AREA (APPROXIMATE)** |
| 1 square inch (sq in, $in^2$) = 6.5 square centimeters ($cm^2$) | 1 square centimeter ($cm^2$) = 0.16 square inch (sq in, $in^2$) |
| 1 square foot (sq ft, $ft^2$) = 0.09 square meter ($m^2$) | 1 square meter ($m^2$) = 1.2 square yards (sq yd, $yd^2$) |
| 1 square yard (sq yd, $yd^2$) = 0.8 square meter ($m^2$) | 1 square kilometer ($km^2$) = 0.4 square mile (sq mi, $mi^2$) |
| 1 square mile (sq mi, $mi^2$) = 2.6 square kilometers ($km^2$) | 10,000 square meters ($m^2$) = 1 hectare (ha) = 2.5 acres |
| 1 acre = 0.4 hectare (he) = 4,000 square meters ($m^2$) | |
| **MASS - WEIGHT (APPROXIMATE)** | **MASS - WEIGHT (APPROXIMATE)** |
| 1 ounce (oz) = 28 grams (gm) | 1 gram (gm) = 0.036 ounce (oz) |
| 1 pound (lb) = 0.45 kilogram (kg) | 1 kilogram (kg) = 2.2 pounds (lb) |
| 1 short ton = 2,000 pounds (lb) = 0.9 tonne (t) | 1 tonne (t) = 1,000 kilograms (kg) |
| | = 1.1 short tons |
| **VOLUME (APPROXIMATE)** | **VOLUME (APPROXIMATE)** |
| 1 teaspoon (tsp) = 5 milliliters (ml) | 1 milliliter (ml) = 0.03 fluid ounce (fl oz) |
| 1 tablespoon (tbsp) = 15 milliliters (ml) | 1 liter (l) = 2.1 pints (pt) |
| 1 fluid ounce (fl oz) = 30 milliliters (ml) | 1 liter (l) = 1.06 quarts (qt) |
| 1 cup (c) = 0.24 liter (l) | 1 liter (l) = 0.26 gallon (gal) |
| 1 pint (pt) = 0.47 liter (l) | |
| 1 quart (qt) = 0.96 liter (l) | |
| 1 gallon (gal) = 3.8 liters (l) | |
| 1 cubic foot (cu ft, $ft^3$) = 0.03 cubic meter ($m^3$) | 1 cubic meter ($m^3$) = 36 cubic feet (cu ft, $ft^3$) |
| 1 cubic yard (cu yd, $yd^3$) = 0.76 cubic meter ($m^3$) | 1 cubic meter ($m^3$) = 1.3 cubic yards (cu yd, $yd^3$) |
| **TEMPERATURE (EXACT)** | **TEMPERATURE (EXACT)** |
| [(x-32)(5/9)] °F = y °C | [(9/5) y + 32] °C = x °F |

## QUICK INCH - CENTIMETER LENGTH CONVERSION

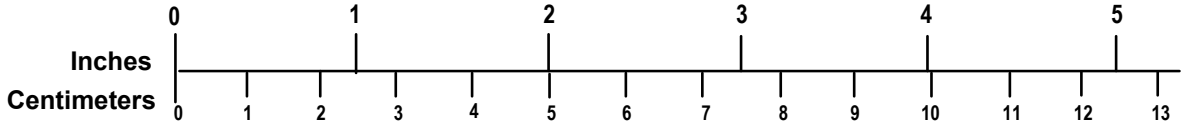


## QUICK FAHRENHEIT - CELSIUS TEMPERATURE CONVERSION

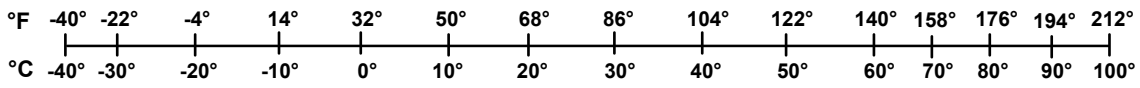


For more exact and or other conversion factors, see NIST Miscellaneous Publication 286, Units of Weights and Measures. Price $2.50 SD Catalog No. C13 10286

Updated 6/17/98

# TABLE OF CONTENTS

## LIST OF FIGURES

## LIST OF TABLES

# EXECUTIVE SUMMARY

On April 4, 2000, at the Federal Railroad Administration's Transportation Technology Center in Pueblo, Colorado, two coupled commuter-rail cars impacted a rigid barrier at 26.25 mph (42 km/h). The impact speed was chosen in order to crush the impacting end of the lead car by approximately 5 ft (1.52 m), as in the single-car test. The kinetic energy in the two-car test was roughly the same as in the single-car test at approximately 3 million ft-lbs.

The cars were instrumented to measure material strain, three-dimensional acceleration of the carbody, vertical displacements of the truck suspension, and longitudinal forces and displacements at the coupler. The structural carbody instrumentation collected 107 channels of data. The cars were also equipped with crash-test dummies in several different seating configurations.

The test was filmed using five high-speed cameras and three video cameras, positioned to focus on the impacting end of the lead car, and the coupled connection between cars. A photometric analysis of the film was performed to calculate the displacement of several target points on the cars during the impact.

Three interior configurations were tested:

1. Forward-facing unrestrained occupants seated in rows, compartmentalized by the forward seat in order to limit the motions of the occupants.

2. Forward-facing restrained occupants with lap and shoulder belts.

3. Rear-facing unrestrained occupants.

The forward-facing unrestrained occupant interior configuration was tested in both the lead and trailing cars, while the forward-facing restrained occupant and rear-facing occupant configurations were tested only in the lead car.

The results from the two-car test have been used to demonstrate that the trailing car serves to reduce the severity of the acceleration/time history of the leading car. The force applied to the leading car by the trailing car minimizes the duration of the initial acceleration peak of the leading car, which reduces the secondary-impact velocity with which an occupant strikes the interior.

The collision-dynamics model predicted the lateral buckling of the cars when there was a small perturbation in the direction of the impact force. However, the model could be improved to better capture the timing of the longitudinal forces transferred through the coupler. From the test data, it appears that the coupler compresses several inches before any significant force develops. Tuning this "gap" in the model will result in a better estimation of the timing of the acceleration peaks of both cars. Also, the model requires more damping at the coupler to minimize the longitudinal oscillation of both cars. In future work, the coupler element will be refined to better estimate the timing in the development of the force at the coupler and to minimize the longitudinal oscillation of the cars. The two-car collision-dynamics model will then be extended to model the train-to-train test scheduled for the fall of 2001.

# 1. INTRODUCTION

The approach taken by the Federal Railroad Administration's (FRA) Office of Research and Development in conducting research into rail-equipment crashworthiness has been to review relevant accidents and identify options for design modifications. Analytic tools and testing techniques are used to evaluate the effectiveness of these options.

As part of this research, computer models have been developed and applied to determine the response of rail equipment in a range of collision scenarios [1, 2, 3, 4, 5, 6]. In-line and oblique train-to-train collisions, as well as grade crossing collisions and rollover events subsequent to derailment have been modeled. The responses of locomotives, cab-cars, and coach cars in a range of collision scenarios have been simulated.

To assess the validity of the models, results of these analyses have been compared with accident data and component test results [7]. While providing useful information and some assurance of the validity of the models, accident data and component and subscale testing all have limitations. There is uncertainty about the initial conditions of any accident: the precise speeds and locations of the two colliding objects are never precisely known. In addition, there is no information on the trajectories of the objects involved in the collision; this information must be inferred from the results of the accidents. The support and loading conditions in component tests can only approximate the actual conditions these components experienced during a collision.

Competing modes of crush (e.g., bending, bulk crushing, and material failure) cannot be consistently scaled for subscale testing [8]. Either one mode of crush must be chosen as the dominant mode and the other modes ignored, or it must be assumed that the simulation accurately scales the competing modes. Full-scale impact tests are necessary in order to know precisely the initial conditions, to measure the trajectories of the equipment during the impact, and to provide the appropriate support conditions for the structure that crushes during the impact, as well as to allow the competing modes of crush to appropriately contribute to the overall crush of the structure.

A series of tests have been planned to measure the crashworthiness performance of conventional-design equipment and to measure the performance of equipment incorporating crushable end structures. These tests are being conducted at the FRA's Transportation Technology Center near Pueblo, Colorado. The collision scenario addressed by these tests is a locomotive-led passenger train colliding with a cab-car-led passenger train on tangent track. The tests planned for each equipment type are:

1. Single-car impact into a fixed barrier.

2. Two-coupled-car impact into a fixed barrier.

3. Cab-car-led train collision with standing locomotive-led train.

Full-scale tests based on a grade-crossing collision scenario are also being developed and will be carried out. These tests are intended to challenge the end structure above the main under-floor structure of the cab-car. In these tests, a heavy rigid object will impact the corner of the cab-car. Two such tests are currently planned, one of a conventional cab-car, as well as a cab-car in

which all the vertical structural elements – the corner posts and collision posts, are tightly tied together with transverse structural elements. These tests are planned for early 2002.

The overall objectives of these tests are to demonstrate the effectiveness of:

- improved-crashworthiness cab-car structural designs,

- improved-crashworthiness coach car structural designs, and

- improved-crashworthiness passenger and operator interior configurations.

To date, the first two tests for conventional-design equipment have been conducted [9, 10, 11, 12, 13, 14, 15]. The third test, to complete the characterization of the performance of conventional-design equipment in an in-line collision, is planned for early 2002. Testing of improved-crashworthiness-design equipment, incorporating crushable end structures, is planned to start in the fall of 2002.

This volume describes the structural crashworthiness of conventional-rail cars. It includes data from Volume II: Summary of Occupant Protection Program, and Volume III: Test Procedures, Instrumentation, and Data [16, 17].

# 2. PLANNED TESTS

Two series of test are planned, one based on a head-on collision scenario, in which a cab car-led train collides with a locomotive-led train, and the second based on a grade-crossing collision scenario, in which a cab car-led train collides with a tractor trailer carrying a coil of sheet steel. Figure 1 shows a schematic representation of the in-line collision scenario. Examples of such collisions include the Prides Crossing, Massachusetts collision between a commuter train and a freight train [18] and the Silver Spring, Maryland collision between a commuter train and an intercity passenger train [19].

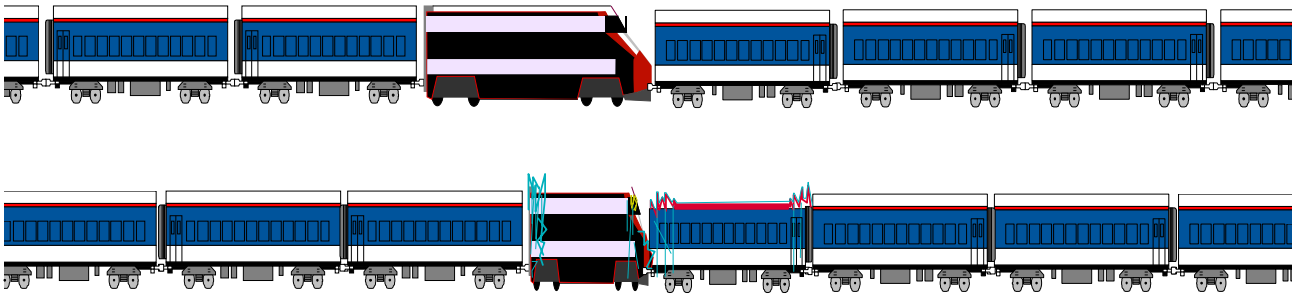

**Figure 1. Schematic of In-Line Collision Scenario**

Figure 2 shows a schematic representation of the grade-crossing collision scenario. Examples of such collisions include the Portage, Indiana collision between a cab-car led commuter train and a tractor-tandem trailer carrying coils of steel [20] and the Yardley, Pennsylvania collision between a cab-car-led commuter train a tractor semi-trailer carrying coils of steel [21].

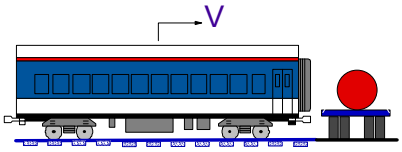


**Figure 2. Schematic of Grade-Crossing Collision Scenario**

The conditions and the sequence of the tests are listed in Table 1. The overall objective of these tests is to demonstrate the effectiveness of improved-crashworthiness equipment. The first series of four tests define the crashworthiness of conventional equipment in the in-line and grade-crossing collision scenarios. The performance of improved-crashworthiness equipment is to be measured in the second series of four tests. This arrangement of the tests allows comparison of the conventional-equipment performance with the performance of improved-crashworthiness equipment. The in-line collision tests are intended to measure the crashworthiness of a single car, then the interactions of two such cars when coupled, and finally the behavior of complete trains, including the interactions of the colliding cars. The requirements for the in-line collision tests are described in Appendix A. The grade-crossing collision tests are intended to measure the effectiveness of the car end structure in preventing intrusion during a grade-crossing collision. The requirements for these tests are currently being developed.

**Table 1. Planned Sequence of Full-scale Passenger-Equipment Impact Tests**

| Test Conditions | Conventional-Design Equipment | Improved-Crashworthiness Design Equipment |
|---|---|---|
| **Single-car impact with fixed barrier** | Test 1 | Test 6 |
| **Two-coupled-car impact with fixed barrier** | Test 2 | Test 7 |
| **Cab car-led train impact with locomotive-led train** | Test 3 | Test 8 |
| **Single-car impact with steel coil** | Test 4 | Test 5 |

## 2.1 SUMMARY DESCRIPTION OF TESTS

Figure 3 shows a schematic of the November 16, 1999 single-car test of a conventional-rail passenger car, which was traveling at 35.1 mph (56.1 km/h) when it impacted the wall [9, 10, 11]. The objectives of this test were to observe the failure modes of the major structural components, to measure the gross motions of the car, to measure the force/crush characteristic, and to evaluate selected occupant-protection strategies.

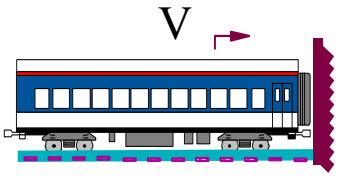


**Figure 3. Schematic of Single-Car Test**

Figure 4 shows a schematic of the April 4, 2000 two-car test of conventional-rail cars, which were traveling at 26.25 mph (42 km/h) when they impacted the wall [15, 16]. This test had the same objectives as the single-car test conducted on November 16, 1999, with the addition of measuring the interactions between the coupled cars.

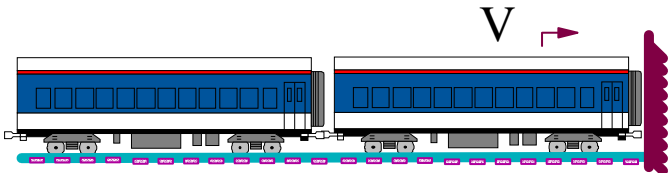


**Figure 4. Schematic of Two-Car Test**

Figure 5 shows a schematic of the train test. In this test, a cab-car-led train impacts a standing locomotive-led train. The locomotive is backed up by ballasted freight cars. This test has the same objectives as the two-car test, with the addition of measuring the interactions between the colliding locomotive and cab-car. This test is planned for early 2002. Simulations of the test are ongoing and the impact speed has yet to be chosen.

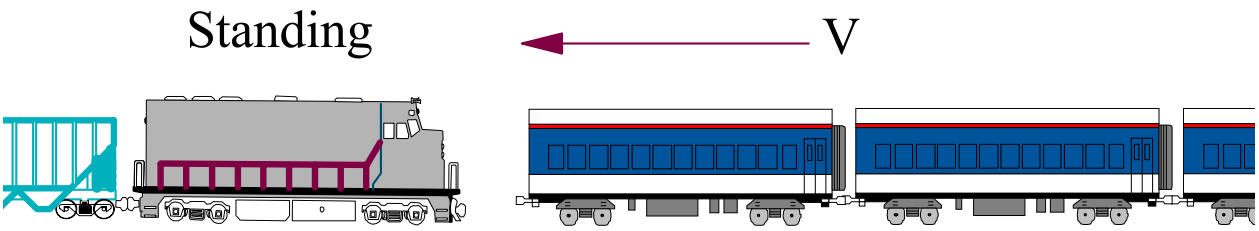


**Figure 5. Schematic of Train-to-Train Test**

Figure 6 shows schematics of the passenger-protection strategies tested in the single-car and two-car tests. All three strategies were tested in the single-car test and in the leading car in the two-car test. The trailing car in the two-car test also tested the forward-facing unrestrained occupant-protection strategy. It is currently planned that all three passenger-protection strategies will be tested in the train-to-train test. However, the locations in the cab-car-led train have not yet been finalized. The principal objective of these tests is to measure the responses of test dummies in several interior configurations.

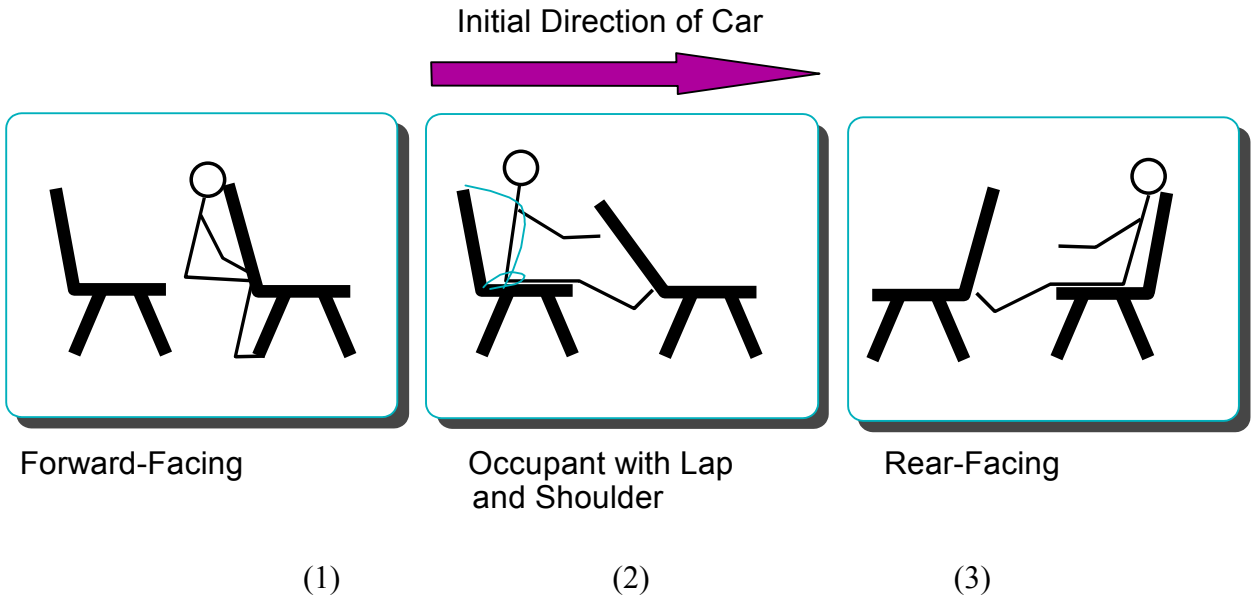


**Figure 6. Schematics of Passenger-Protection Strategies**

Figure 7 shows a schematic of the locomotive operator's interior environment to be tested during the train-to-train test. The objective of this test is principally to observe the kinematics of the test dummy, as well as to measure the test-dummy response and evaluate the potential for occupant injury.

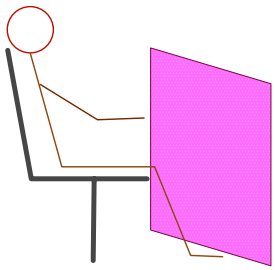

**Figure 7. Schematic of Locomotive Operator Interior Test**

Table 2 summarizes the critical measurements for each of the three tests. While the overall objective of these tests is to demonstrate the effectiveness of improved-crashworthiness equipment, the test data are also being used for comparison with analyses and modeling results. The measurements will be used to refine these analyses' approaches and models, and to ensure that the factors influencing the response of the equipment and test dummies are taken into account. The table lists the measurements that are critical to ensuring the appropriate modeling and analysis of the equipment and test dummies.

**Table 2. Test Descriptions and Critical Measurements**

| Test Description | Critical Measurement |
|---|---|
| **Single-Car Test** | - Dynamic crush force<br>- Loss of occupant volume<br>- Occupant volume deceleration<br>- Effectiveness of compartmentalization, rear-facing seats, and seats with lap and shoulder belts |
| **Two-Car Test** | - "Sawtooth" lateral buckling of coupled cars<br>- Influence of trailing car on maximum occupant volume deceleration<br>- Effectiveness of compartmentalization, rear-facing seats, and seats with lap and shoulder belts |
| **Train-to-Train Test** | - Lateral buckling of coupled cars<br>- Override of colliding cars<br>- Effectiveness of compartmentalization, rear-facing seats, and seats with lap and shoulder belts<br>- Measurement of operator secondary-collision environment |

# 3. TWO-CAR TEST DESCRIPTION

Two coupled commuter-rail cars impacted a rigid barrier at 26.25 mph (42 km/h). The impact speed was chosen in order to crush the impacting end of the lead car by approximately 5 feet (1.52 m), as in the single-car test. The kinetic energy in the two-car test was roughly the same as in the single-car test (~ 3 million ft-lbs.).

Both cars were Pioneer cars, designed and built by the Budd Company [22]. A locomotive was used to push the coupled cars down a constant-gradient slope and release them such that they impacted the wall at the desired speed.

The cars were stripped of the original passenger seats and some auxiliary equipment to make room for the interior seat/occupant experiments.

About 10,000 lbs (4,500 kg) of ballast was added to the cars, resulting in a total weight of approximately 75,000 lbs (33,750 kg) for each car. The weight of a fully-equipped car used in passenger service is about 100,000 lbs (45,000 kg). Conducting the test with the lighter vehicle results in less damage than would occur in a test with a fully-equipped vehicle at the same speed.

The cars were instrumented to measure material strain, three-dimensional acceleration of the carbody, vertical displacements of the truck suspension, and longitudinal forces and displacements at the coupler. The structural carbody instrumentation collected 107 channels of data. The cars were also equipped with crash-test dummies in several different seating configurations.

The test was filmed using five high-speed cameras and three video cameras, positioned to focus on the impacting end of the lead car, and the coupled connection between cars. A photometric analysis of the film was performed to calculate the displacement of several target points on the cars during the impact.

Figure 8 shows the interior experiments carried out as part of the two-car test. Three interior configurations were tested:

1. Forward-facing unrestrained occupants seated in rows, compartmentalized by the forward seat in order to limit the motions of the occupants.

2. Forward-facing restrained occupants with lap and shoulder belts.

3. Rear-facing unrestrained occupants.

The forward-facing unrestrained occupant interior configuration was tested in both the lead and trailing cars, while the forward-facing restrained occupant and rear-facing occupant configurations were tested only in the lead car. Figure 8 shows the placement of the interior configurations in the two-car tests.

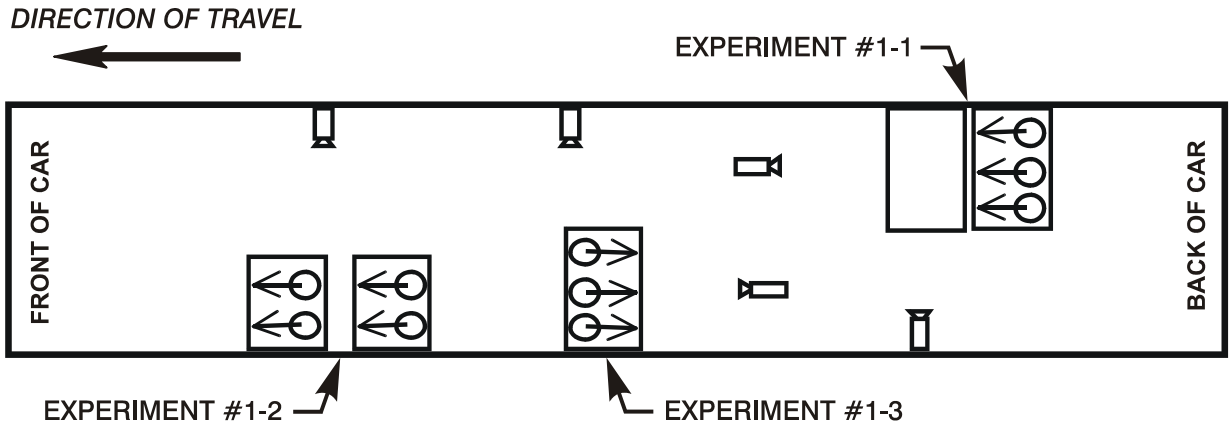


**Figure 8a. Location of Interior Test Configurations in Leading Car**

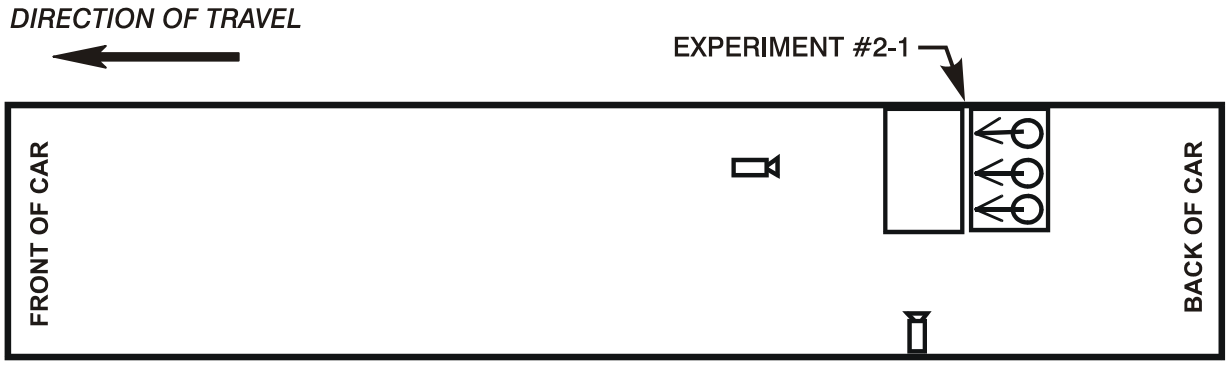


**Figure 8b. Location of Interior Test Configurations in Trailing Car**

## 3.1 MODELING APPROACH

The flow chart in Figure 9 illustrates the approach used to model the full-scale collision tests. Finite-element models provide initial estimates for the force/crush behavior of discrete nonlinear springs in the collision-dynamics analysis. A collision-dynamics model can then be used to estimate the forces and displacements in full-scale testing as well as the acceleration environment for interior occupant analysis. Test measurements are used to modify the collision-dynamics model parameters to increase the fidelity of estimated behavior. The validated collision-dynamics model can then be employed to estimate crashworthiness behavior under collision conditions for which test data is not available.

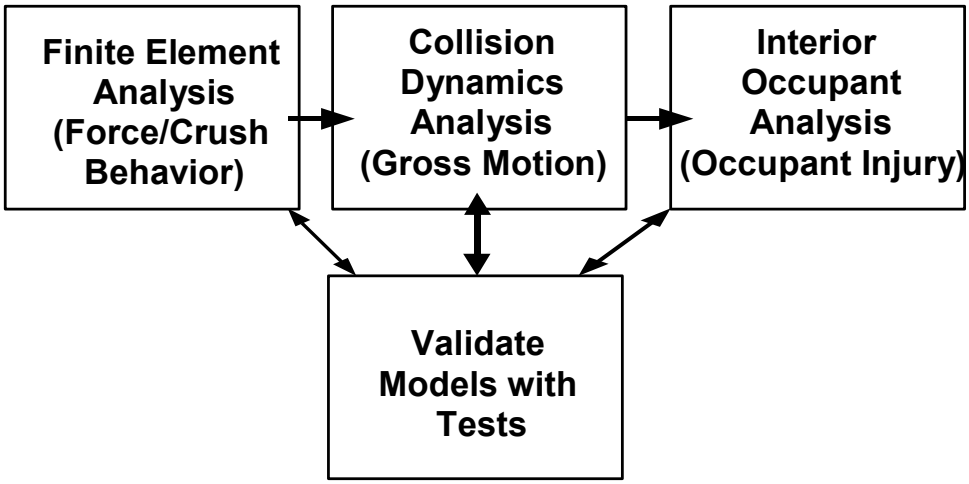


**Figure 9. Modeling Approach**

Prior to the full-scale impact tests, the force-crush behavior of the vehicle end structure was estimated by exercising a detailed finite-element model of a single passenger-rail vehicle (Figure 10) [23]. The model represents an Amfleet car, built by the Budd Company. The geometry and materials of the primary structural members (i.e., draft sill, center sill, side sills, cant rails, collision and corner posts) are very similar in both the Amfleet and Pioneer cars. The finite-element model did not account for the suspension characteristics or the vehicle/track interaction.

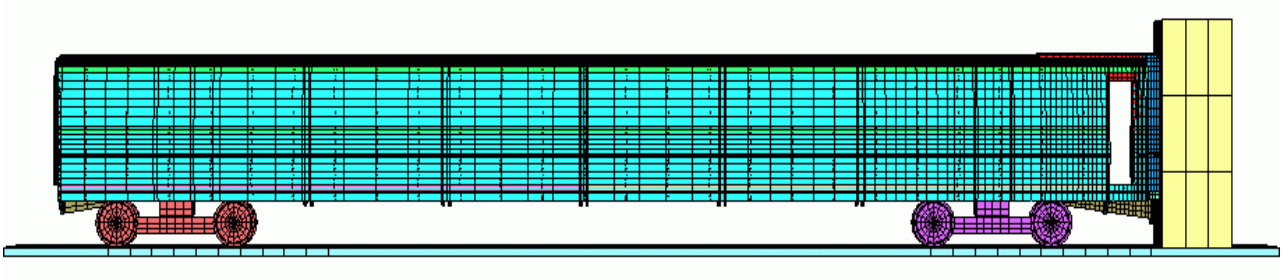

**Figure 10. Finite-Element Model**

A lumped-mass collision-dynamics model (Figure 11a) was used to estimate the gross motion of the car and the collapse of the end structure. The collision-dynamics model uses a series of discrete masses connected by non-linear springs and dampers. It runs much more quickly than the finite-element model and the force/crush behavior is more readily modified to better estimate the gross motion of the car during the impact test.

Following the single-car test, the collision-dynamics model was modified to better represent the test results. To estimate the results of the two-car test, a trailing car was added to the model (Figure 11b). The trailing car and coupled connection between the cars was adapted from a collision-dynamics model previously developed to investigate lateral buckling [4]. Following the two-car test, the model of the impacting car was modified to better reflect the results of both tests. The impacting car is identical in the single-car and two-car models. This report compares the two-car test data with the results of the corresponding collision-dynamics model.

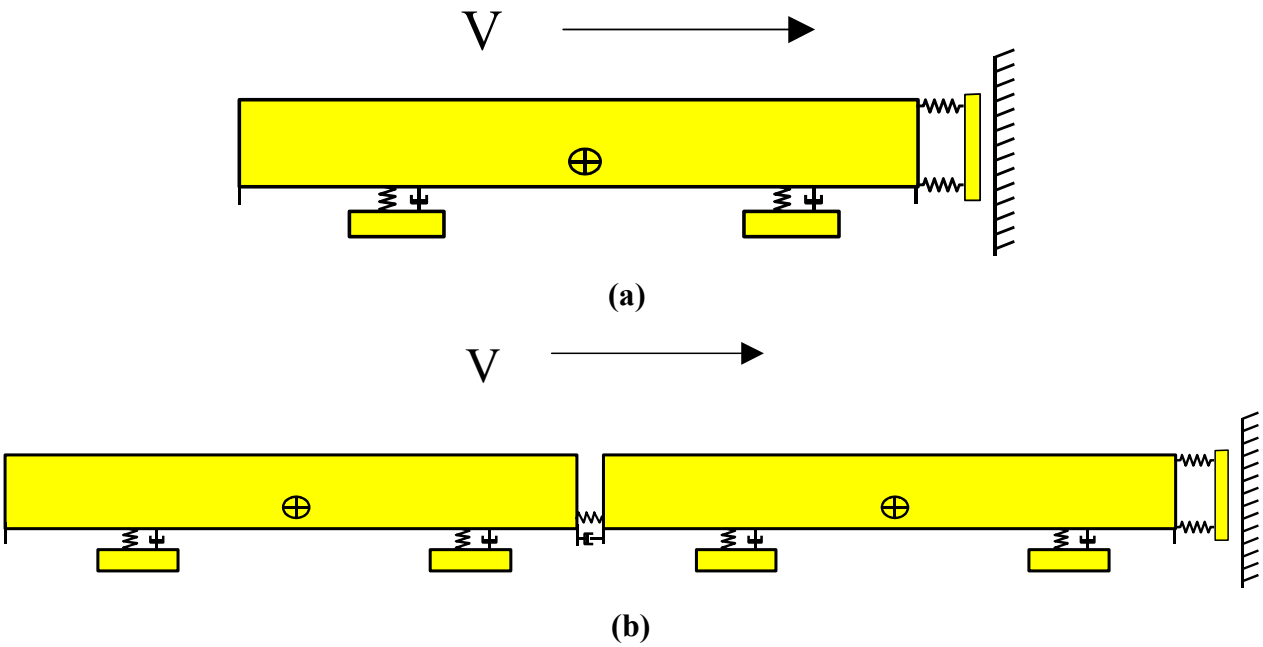


**Figure 11. Schematic of Collision-Dynamics Model**

The impacting car in both collision-dynamics models consists of four rigid masses that represent the front portion of the vehicle, the trucks and the main carbody. The trailing car in the two-car model does not have a separate mass representing the leading end of the vehicle, because little crush was expected between the two cars. The model is capable of three-dimensional motion since each mass is allowed three translational and three rotational degrees of freedom. However, for this study the masses representing the front end and the main carbody were constrained to translate longitudinally with respect to one another. Non linear springs and dampers that represent the crushable end structure, the truck/carbody suspension, and the coupler, were used to connect the masses. For more detail on the parameters used in the model, see Appendix B.

The carbody accelerations calculated with the collision-dynamics model are used as input to an interior seat/occupant model (Figure 12). This model also uses the force-deflection behavior of passenger seats that has been previously calculated during static tests [24]. Using the interior-dynamics model, the forces and accelerations experienced by occupants in a collision can be estimated. Using these forces and accelerations, the degree of injuries sustained to the head, neck, chest, and femur can be calculated. The injury criteria can be used to evaluate and compare the level of protection provided to occupants under different collision conditions.

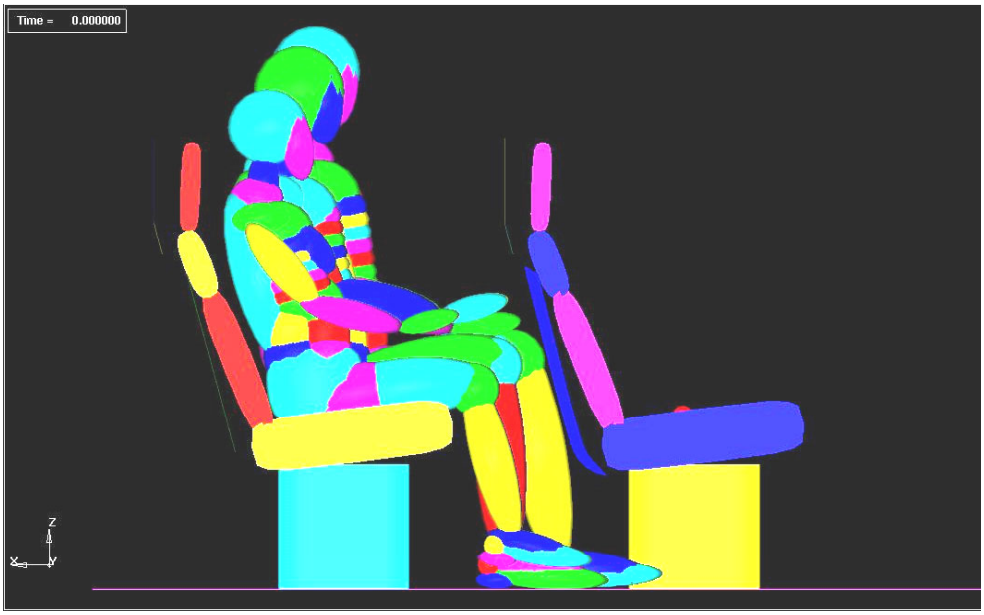


**Figure 12. Interior Seat/Occupant Model**

## 3.2 PROCESSING OF TEST DATA

The total force on the wall as a function of time was estimated by multiplying the mass of each car with the acceleration of each car. The sum of the two products is the estimated force/time history at the wall:

$$F_t(t) = M_1 * A_1(t) + M_2 * A_2(t) \qquad (1)$$

The displacement/time history of the leading vehicle was calculated by integrating the acceleration/time history of the leading vehicle twice. The force was plotted against the double-integrated displacement/time history to represent the force on the wall as a function of crush of the impacting vehicle.

The raw accelerometer data contained components attributable to carbody flexibility. The data was filtered in order to remove the high-frequency content while retaining the essential rigid body motion of the carbody. The filtered accelerometer data was then integrated to calculate the corresponding velocity and displacement data.

The choice of cut-off frequency has a significant effect on the integrated displacement data. Comparison of the integrated displacement data and the photometric displacement data was used to define the appropriate cut-off value. The accelerometer nearest the center of gravity (CG) was chosen to represent the gross longitudinal motion of the vehicle. Displacement/time histories integrated from this accelerometer and filtered at several frequencies are plotted in Figure 13, along with the photometric displacement data for comparison.

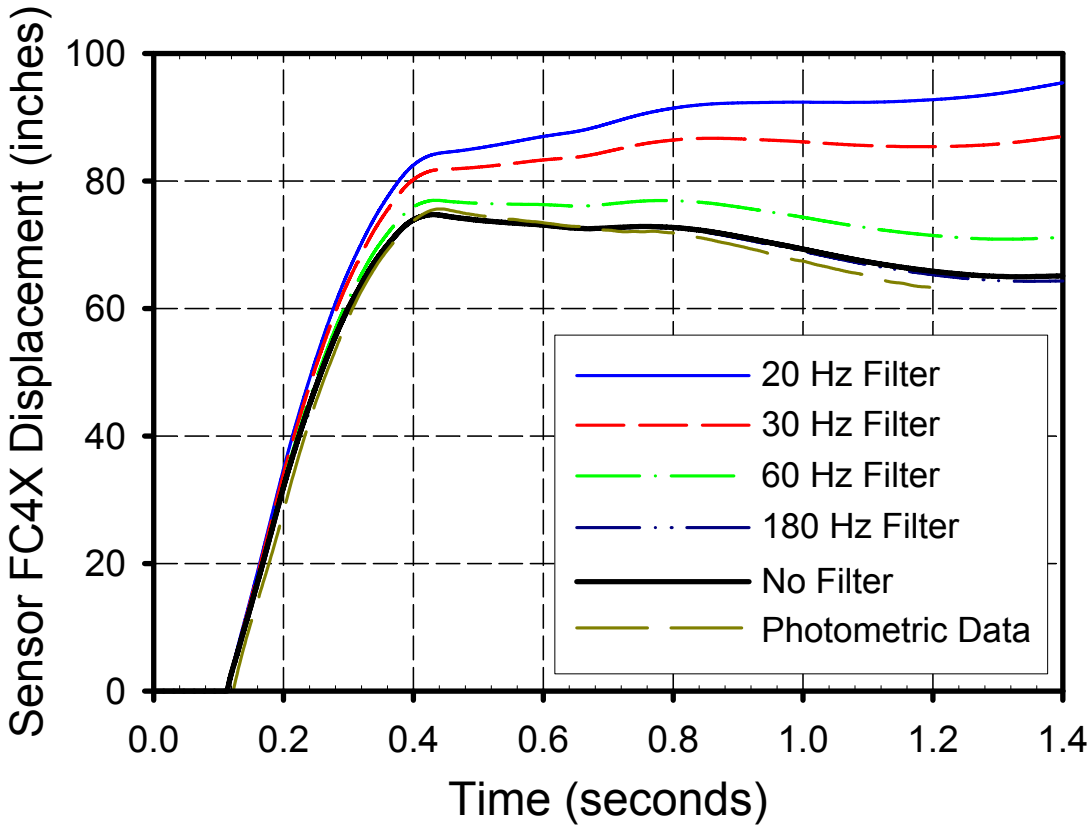


**Figure 13. Comparison of Effect of Filtering Frequency on Displacement/Time History**

To minimize the error in integrated displacement, the accelerometer signal was processed in accordance with SAE J211.1 (Surface Vehicle Recommended Practice – Instrumentation for Impact Tests). To compute the acceleration, a CFC 60 Butterworth 4-pole phaseless digital filter was used. To compute the displacement, a CFC 180 Butterworth 4-pole phaseless digital filter was used. The difference in the displacement/time histories for the 180-Hz data and the unfiltered data is negligible. The acceleration predictions from the collision-dynamics analysis were filtered in the same manner.

Accelerometer data from a single accelerometer from the single-car test had been filtered using a 30-Hz low-pass filter [9]. After reviewing all of the accelerometers from the single- and two-car tests and SAE J211.1, it was apparent that error in the integrated displacement data had been introduced by over-filtering the acceleration. The single-car test data was reprocessed in accordance with J211.1. The corrected results are presented in Appendix C. The peak acceleration is approximately 14 Gs when a CFC 30 is used in filtering the accelerations, versus a peak of about 38 Gs that results from using a CFC 60 filter. As discussed in the next section, the peak acceleration is not particularly significant in terms of the collision environment experienced by an unrestrained occupant.

An appropriate accelerometer had to be selected to represent each car. All the 11 filtered longitudinal acceleration traces were reviewed (see Figure 14 and Figure 15 for accelerometer locations). There is a time delay in the signal for locations that are further towards the rear of each car. Elastic response of the carbody has the largest effect at the rear of each car. A simple average of all of the accelerometers masks the relevant detail from the signal.

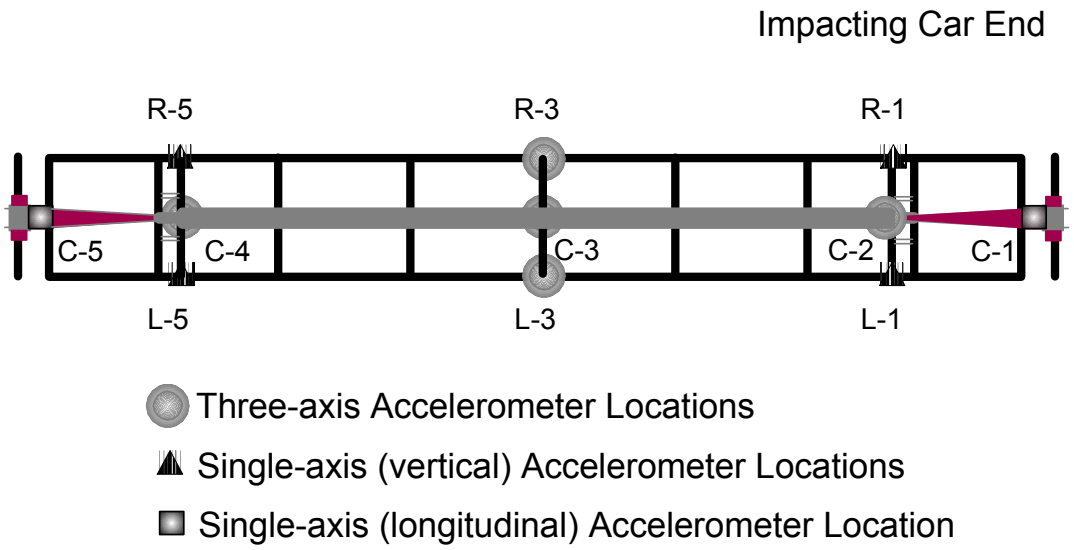


**Figure 14. Leading Car Accelerometer Locations**

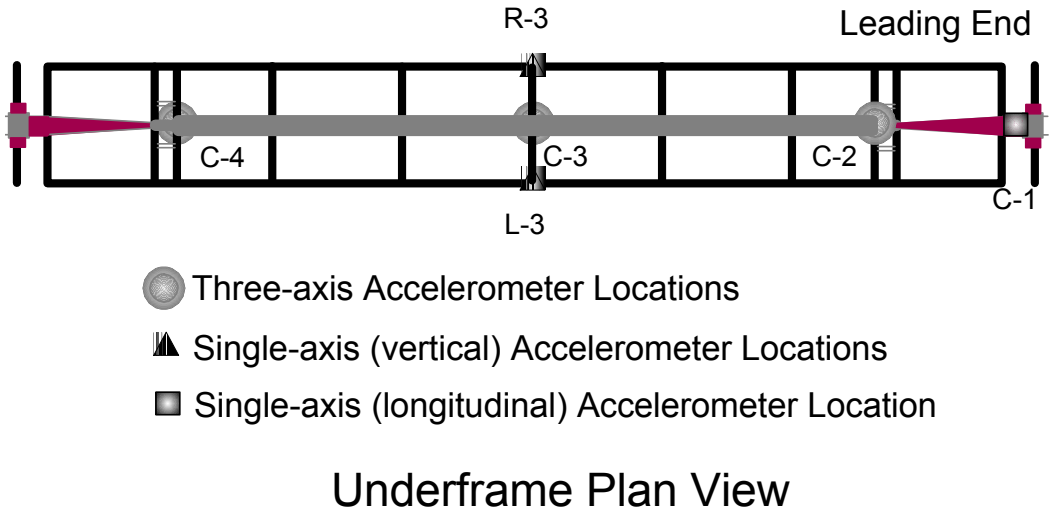


**Figure 15. Trailing Car Accelerometer Locations**

The accelerometers labeled C-3 in both the leading and trailing cars were used to represent the longitudinal motion of the respective carbodies. These accelerometers were both located on the center sill at the longitudinal center of the car, near the CG. Due to this mounting location, it is expected that the data would be less affected by carbody pitch and yaw than data from accelerometers located further away from the CG.

# 4. TEST AND ANALYSIS RESULTS

## 4.1 FORCE/CRUSH BEHAVIOR

During the two-car impact test, most of the damage occurred at the impacting end of the lead car, which crushed approximately 6 ft (1.8 m) (see Figure 16 and Figure 17 for pre- and post-test photos of the impacting end of the lead car). There was little damage at the coupled connection between the cars. The peak force between the lead car and the impact wall was nearly 2.5 million pounds, with a steady force of approximately 500,000 lbs (225,000 kg). Figure 18 shows the comparison of the force/crush behavior measured during the test and calculated with the collision-dynamics analysis. The collision-dynamics analysis matches the peak force, timing, steady value, and total crush very well. The estimated peak force on the wall is a function of the acceleration of the two-car bodies, which is influenced by the CFC used to filter the acceleration.

Both the single-car and two-car collision-dynamics models were modified subsequent to the two-car test to further improve the results of each model. The test and analysis data for both tests compares well, in terms of the timing of the peak force, the average force, and the total crush.

For comparison, the force/crush behavior from the single-car test is plotted with the two-car test data in Figure 19. The curves from both tests are very similar in terms of peak force and steady force. Total crush in the two-car test is about 10 inches greater, since the kinetic energy was slightly higher than in the single-car test.

As an additional check that the force and displacement data were calculated properly, the energy absorbed during the collision was calculated by integrating the force/crush curve, and comparing the results to the total energy available (i.e., $\frac{1}{2}*M*V^2$). While the respective test and analysis curves are not identical, the total energy absorbed (i.e., the area under each of the curves) varies by less than 1 percent.

**Figure 16. Photo of Impact End of Leading Car Prior to Two-Car Impact Test**

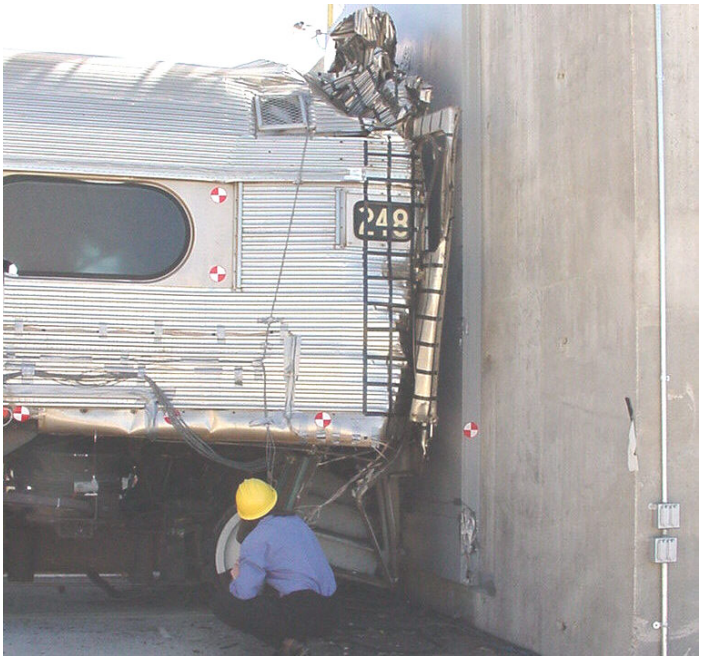

**Figure 17. Photo of Impact End of Leading Car After Two-Car Impact Test**

The mode of crush of the draft sill was quite different between the two tests. In the single-car test, the draft sill split along the longitudinal seam welds of the box. The top plate folded up in the vertical plane, and the two side plates folded up in the lateral plane. The tapered section nearest the body bolster was intact. In the two-car test, the widest part of the draft sill at the end of the car stayed relatively intact, pushing back on the tapered section of the draft sill, which buckled extensively. Although the mode of crush of the draft sills was different in each test, the force/crush behavior of the car was similar in both tests.

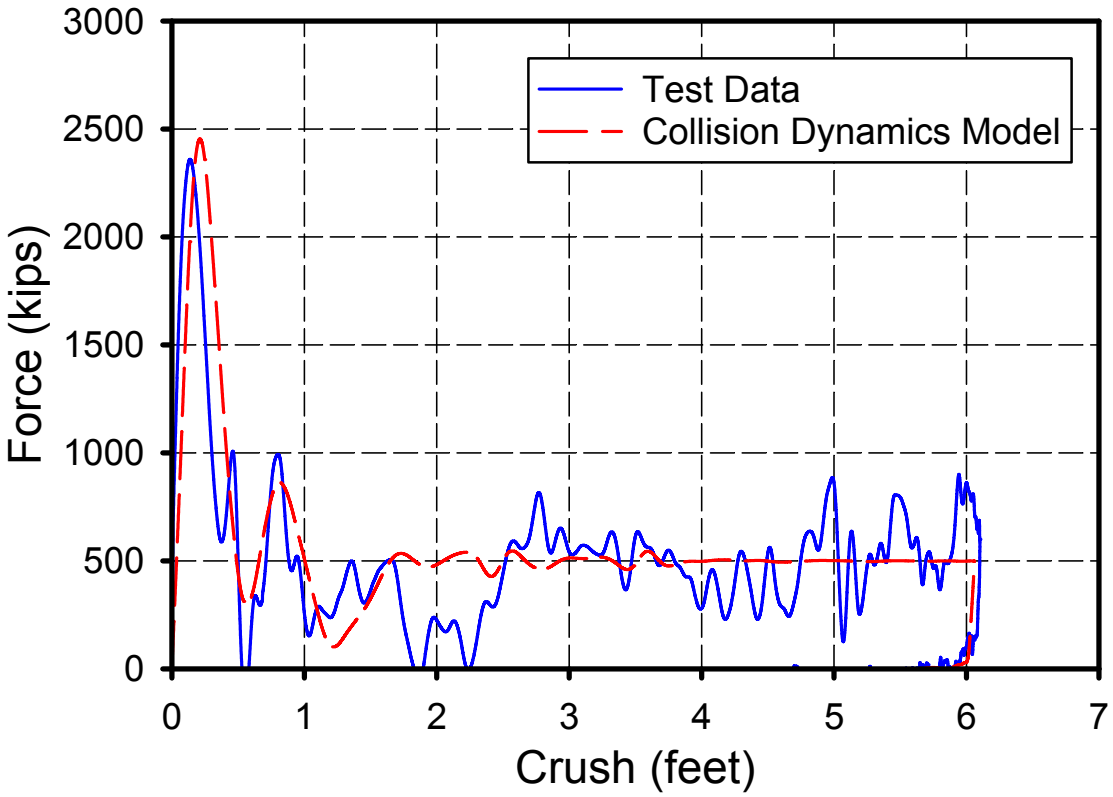


**Figure 18. Comparison of Force/Crush Behavior from Two-Car Impact Test**

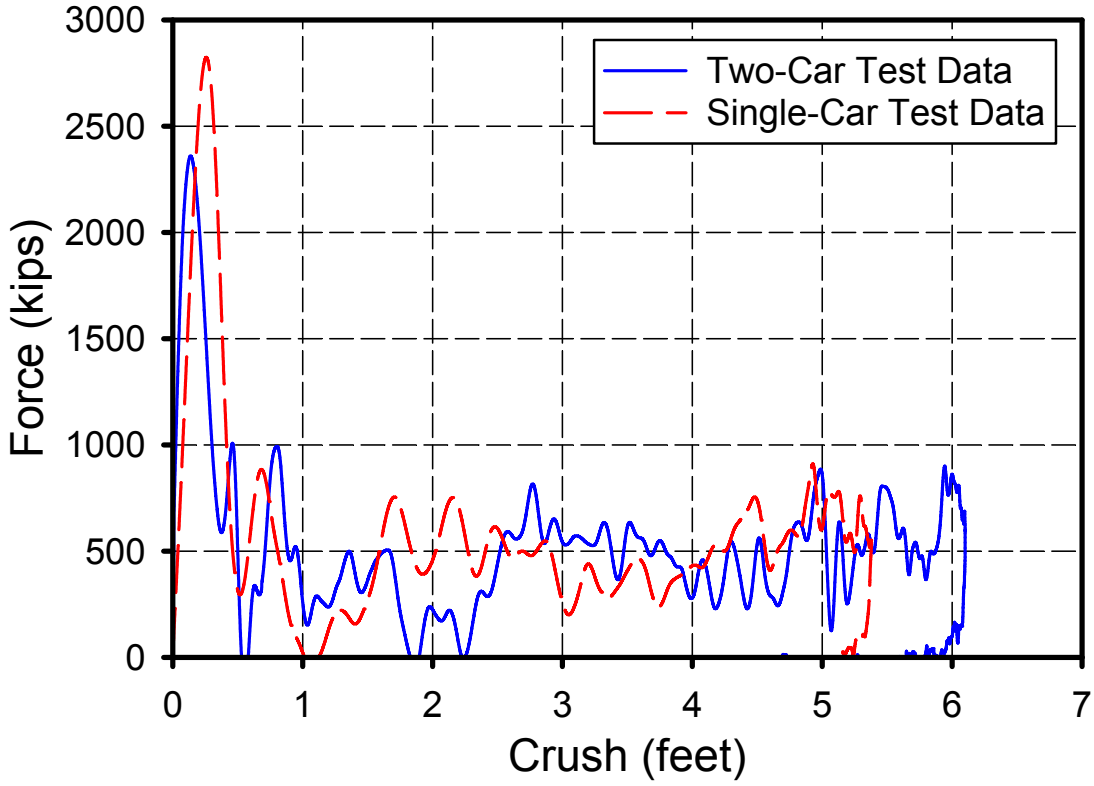


**Figure 19. Comparison of Force/Crush Behavior from Single-Car and Two-Car Impact Tests**

## 4.2 GROSS MOTION

The two cars remained coupled during the test, but buckled in a saw-tooth mode as intended. The maximum lateral displacement between the cars during the collision was approximately 30 inches, with a final lateral displacement of 15 inches following the test (see Figure 20). The left rail buckled under the lateral load from the front truck of the trailing car, allowing the right wheels of the front truck of the trailing car to drop between the rails.

The impacting end of the leading car rose about 6 inches during the impact, and came to rest with all wheels from both trucks still on the track.


**Figure 20. Photo of Coupled Connection After Two-Car Impact Test**

The lateral carbody accelerations in the two-car test were small, with high-frequency peaks on the order of 2 to 3 Gs. Vertically, the high-frequency peaks were about 5 Gs during the first 0.3 seconds, with a good deal of elastic vibration. After the elastic vibration died out, the acceleration had a sinusoidal pattern at about 6 Hz with an amplitude of 2 to 3 Gs, that damped out after about three cycles.

## 4.3 OCCUPANT ENVIRONMENT

The occupant environment during a collision is defined as the interior configuration and its associated engineering details, and the deceleration imparted to that configuration. During an in-line train collision, the greatest decelerations are longitudinal. However, significant lateral and vertical accelerations that influence the kinematics of the occupants can arise. This section describes the longitudinal, vertical, and lateral accelerations measured during the two-car test. The crash pulses described here were measured at the center of the floor in both the leading and trailing cars. (Reference 16 describes the results of the occupant-protection experiments conducted as part of the two-car impact test.)

The deceleration/time histories from the leading and trailing cars are shown in Figure 21 and Figure 22, respectively, along with the corresponding data from the collision-dynamics analysis. Although the estimated force acting on the wall was similar in both tests, the accelerations of the cars were very different. The longitudinal deceleration/time history, or crash pulse, of the lead car is characterized by a high initial peak with a short duration, followed by oscillations around zero, followed by a fairly steady deceleration. The initial peak is due to the high load required to initiate collapse of the car structure impacting the wall, the oscillations about zero are due to the impact of the trailing car with the leading car, and the final steady deceleration is both cars riding down the collision as the structure of the lead car crushes. The trailing car in the two-car test acts to minimize the acceleration of the lead car during the first 100 milliseconds. While the lead car is decelerating due to the impact with the wall, the trailing car is simultaneously trying to accelerate the lead car. The peak acceleration of the trailing car is much less than that of the leading car because it is effectively buffered by the crushing of the leading car. The average deceleration for the lead car over the 0.4 seconds shown is 3.1 Gs, while it is 3.2 Gs for the trailing car.

Qualitatively, the model predicts the details of the decelerations very closely. The collision-dynamics analysis predicts a high initial peak followed by a reversal of the acceleration for the lead car, just as measured in the test. The overall shape of the acceleration/time history for the trailing car in the collision-dynamics analysis compares favorably with the test measurement. The only significant difference in the test and collision-dynamics analysis is in the timing of the peaks and the oscillation as shown in Figures 21 and 22. This difference is attributable to the representation of the coupler.

For comparison, the plot shown in Figure 21 includes the 8 G-triangular pulse used in previous sled testing [24]. The 8 G crash was developed from an analytic model of a collision between two locomotive-led trains. The 8 G crash pulse approximates the deceleration predicted with that model of the first coach behind a locomotive during a 70 mph (112 km/h) collision. This pulse has a significantly different characteristic from the longitudinal decelerations measured during the test. The average value of this pulse, however, is 4 Gs, which is greater than averages for the pulses measured during the test. The influence of the shape, or characteristic on the likelihood of injury depends upon the interior configuration. The average deceleration is greatest for the 8 G-triangular pulse and consequently, for unrestrained forward-facing occupants seated in rows, the likelihood of injury is probably greatest for this pulse. For restrained occupants the principal concern is the loads imparted to the neck. Since, in effect, the occupant “impacts” the restraints earlier for the crash pulse measured in the leading car (owing to its initial peak) than for the other two crash pulses, it is expected that the leading-car crash pulse is most likely to result in injury. Similarly, for rear-facing occupants, the crash pulse of the leading car is likely to be most severe because of the initial peak.

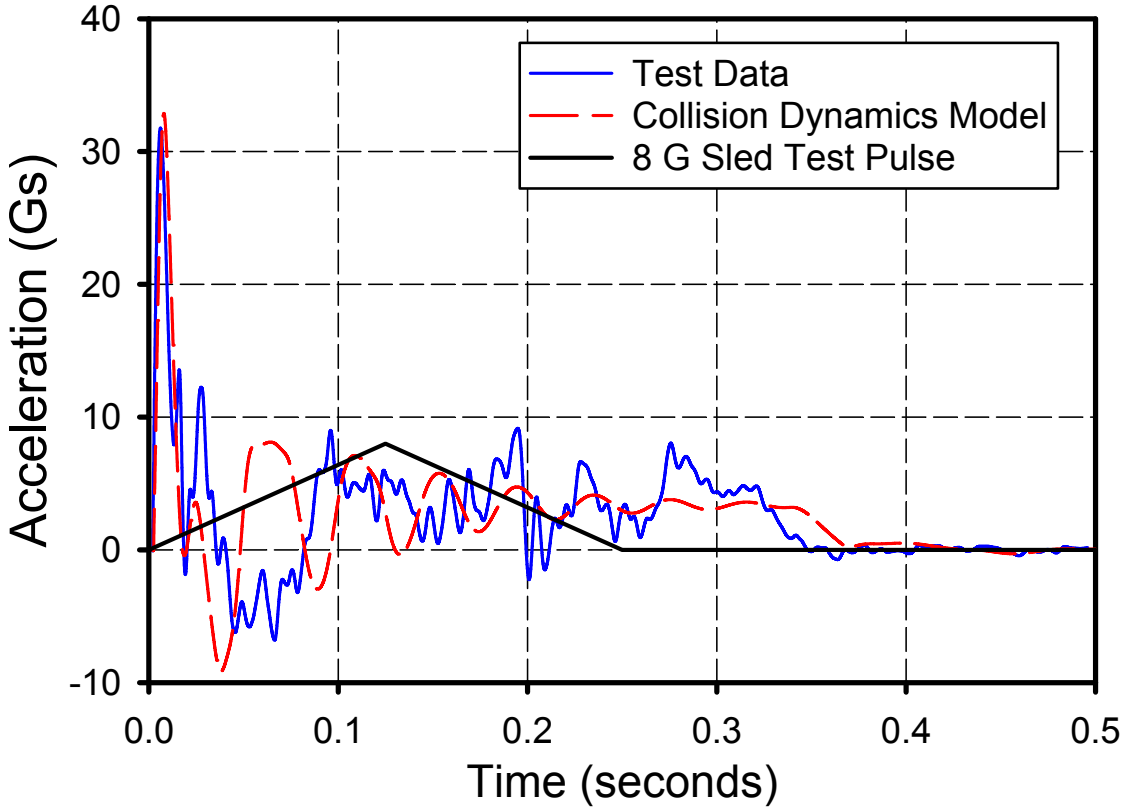


**Figure 21. Comparison of Longitudinal Accelerations of CG of Leading Car from Two-Car Test**

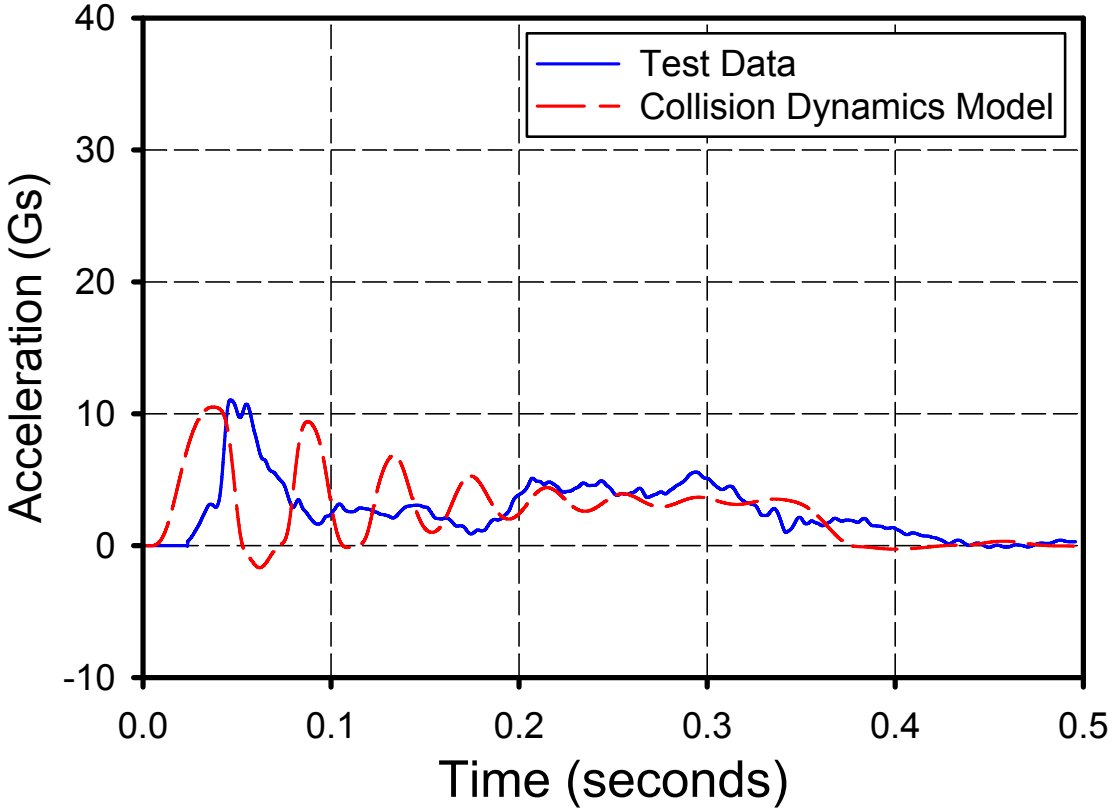


**Figure 22. Comparison of Longitudinal Accelerations of CG of Trailing Car from Two-Car Test**

Figures 23a and 23b shows the vertical accelerations of the leading and trailing cars in the two-car test, respectively. Both plots show the vertical accelerations at the leading body bolster, at the center of the floor, and at the trailing body bolster. The measurements include the influence of the pitch and bounce of the cars, as well as the elastic vibrations of the carbodies and accelerometer mountings.

Observation of the high-speed film taken during the test indicates that both cars essentially rotated about a point near the trailing body bolster while they pitched upward. This motion resulted in a maximum elevation of approximately 6 inches (15 cm) at the front body bolster for the leading car, and 3 inches (7.5 cm) for the trailing car. The elastic vibrations of the carbody dominate the vertical accelerations of both cars – the acceleration signatures appear to oscillate about zero for the duration of the impact.

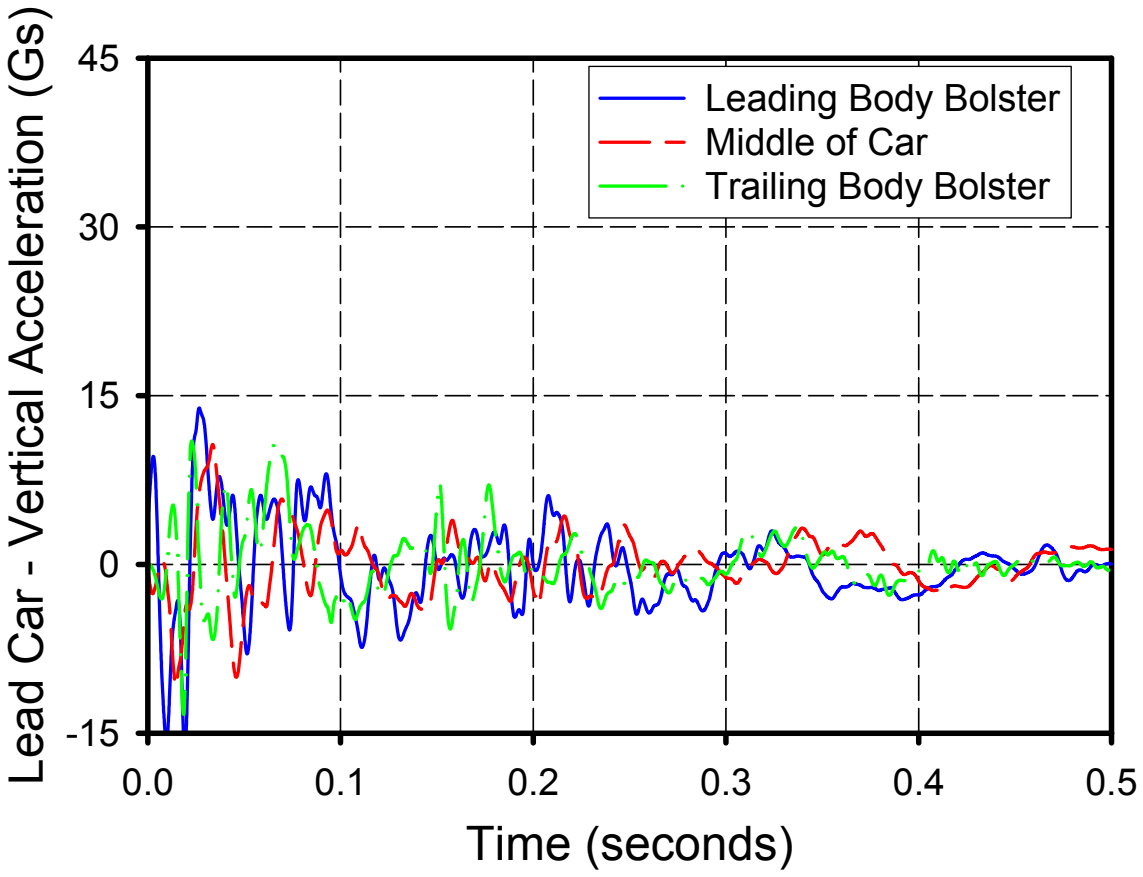


**Figure 23a. Vertical Carbody Accelerations vs. Time, Leading Car**

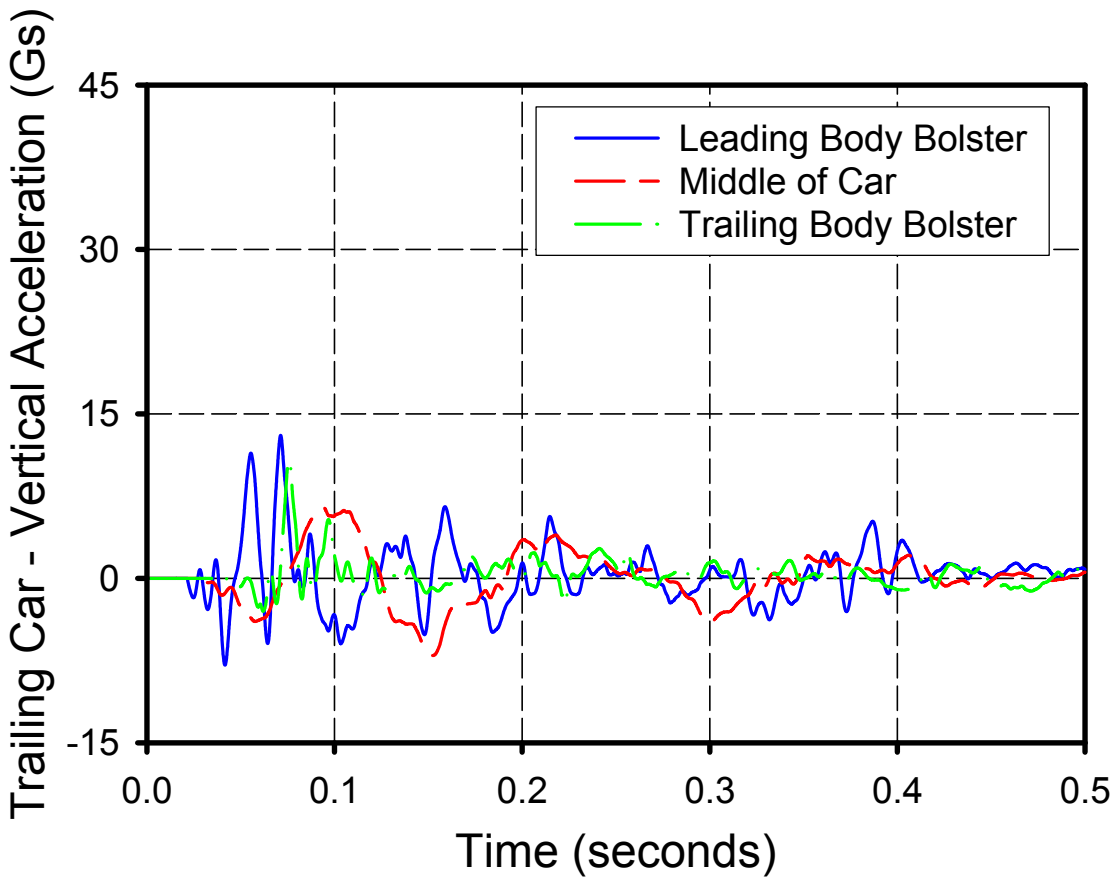


**Figure 23b. Vertical Carbody Accelerations vs. Time, Trailing Car**

The lateral accelerations measured in the leading and trailing cars in the two-car test are shown in Figures 24a and 24b, respectively. The lateral acceleration for the leading car has an initial peak whose timing corresponds with the impact from the trailing car. The trailing-car lateral acceleration is smaller than the leading-car lateral acceleration. Similar to the vertical-acceleration measurements, the lateral-acceleration measurements include the influence of the yaw and sway of the cars, as well as the elastic vibrations of the carbodies and accelerometer mountings. During the test, both cars yawed in a counterclockwise direction, which resulted in a "sawtooth" lateral buckle of the coupled cars. From the high-speed film, both cars apparently yawed about their trailing body bolster.

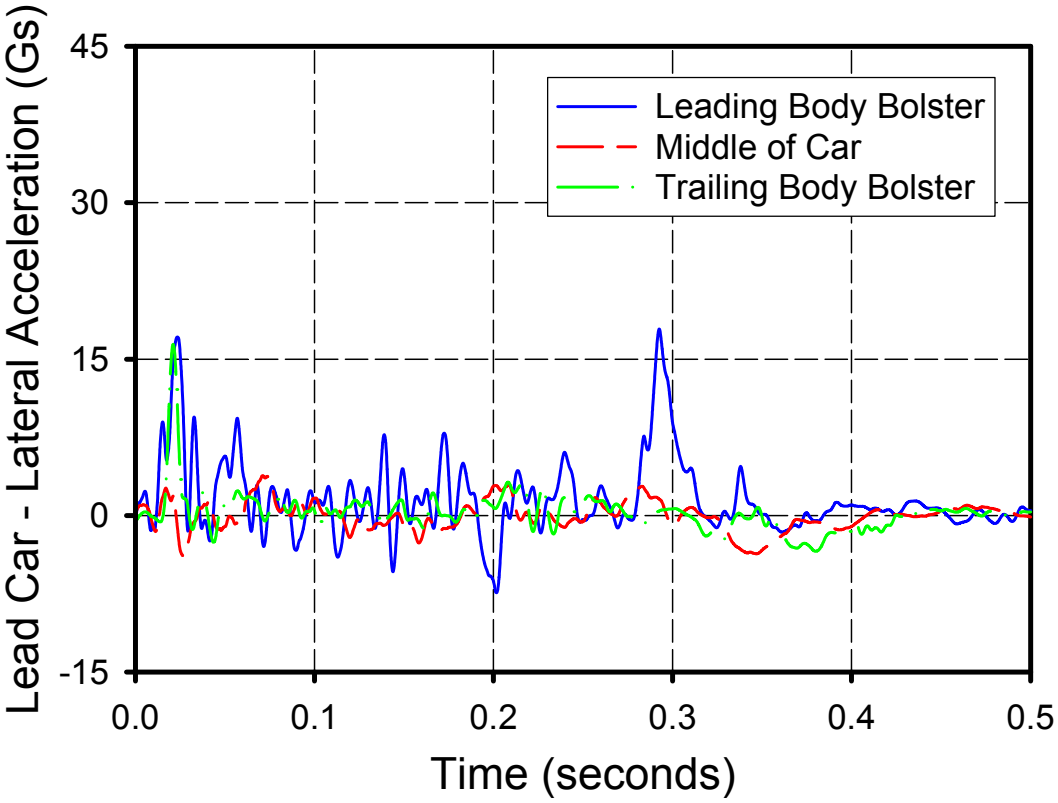


**Figure 24a. Lateral Carbody Accelerations vs. Time, Leading Car**

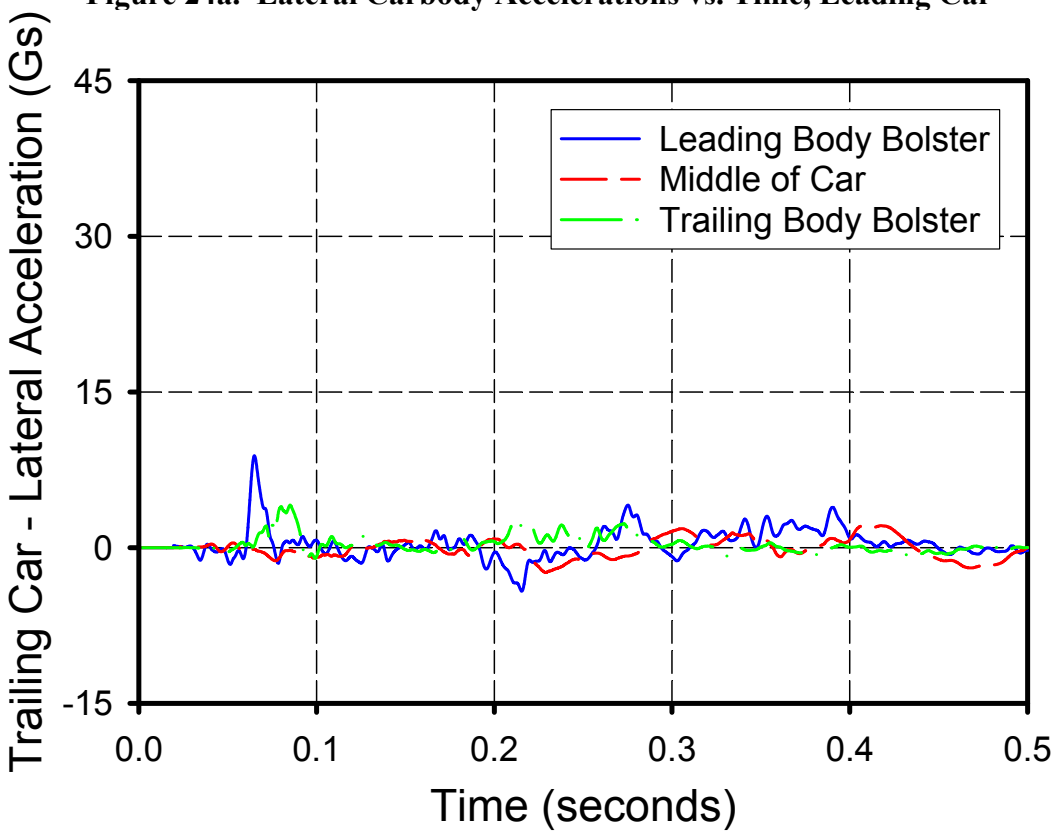


**Figure 24b. Lateral Carbody Accelerations vs. Time, Trailing Car**

Table 3 lists the average longitudinal, vertical, and lateral accelerations in the leading and trailing cars during the two-car test. It can be seen in the table that except for the lead body bolster sensors, the longitudinal deceleration is nearly an order of magnitude larger than lateral and vertical accelerations. For the rear-facing and restrained occupants, the influence of the lateral and vertical accelerations on the occupant response, and consequently, their influence on the likelihood of injury, is expected to be small. For the rear-facing occupants, the longitudinal deceleration, in combination with the friction between the occupant and seat, prevents much lateral and vertical motion of the occupants during the most severe portion of the primary impact. For the restrained occupants, the restraints prevent much of the vertical and lateral motion of the occupants. For unrestrained occupants that travel some distance before their secondary impact, however, the lateral and vertical motions of the car may potentially influence the occupant motion and influence their likelihood of injury. In particular, for unrestrained forward-facing occupants seated in rows, there is a possibility of relative vertical and lateral displacement between the seat ahead and the occupant. These displacements may result in an occupant's head missing the seat ahead of them, and the neck impacting the top of the seatback. If this does occur, then there is potential for high neck loads and consequent injury.

**Table 3. Average Longitudinal, Vertical, and Lateral Accelerations, Leading and Trailing Cars**

| Average Acceleration 0 to 0.4 seconds | Leading Car | Trailing Car | 8 G-Pulse[1] |
|---|---|---|---|
| Longitudinal | 3.1 G | 3.2 G | 4 G |
| Vertical, Leading Body Bolster | 2.37 G | 0.19 G | NA |
| Vertical, Middle of Car | 0.11 G | 0.04 G | NA |
| Vertical, Trailing Body Bolster | 0.16 G | 0.46 G | NA |
| Lateral, Leading Body Bolster | 1.88 G | 0.44 G | NA |
| Lateral, Middle of Car | -0.08 G | -0.04 G | NA |
| Lateral, Trailing Body Bolster | 0.34 G | 0.46 G | NA |

Figure 25 shows a plot of the time-history of the displacement, relative to the interior of the cars, of the head of an unrestrained forward-facing occupant. This plot is derived from the test data and the assumption that the occupant is in free-flight during the impact [3]. The distance from the front of an occupant's head to the seatback ahead of them is approximately 2 feet (60 cm) for typical commuter-seat spacing, and approximately 2.5 feet (76 cm) in typical intercity-seat spacing. The plot indicates that the head of a forward-facing unrestrained occupant seated in rows of seats would impact the back of the seat ahead at 0.18 to 0.20 seconds after the leading car impacts the wall; the secondary impacts occurs at about the same time in both the trailing and leading cars.

[1] Averaged over 0.25 seconds.

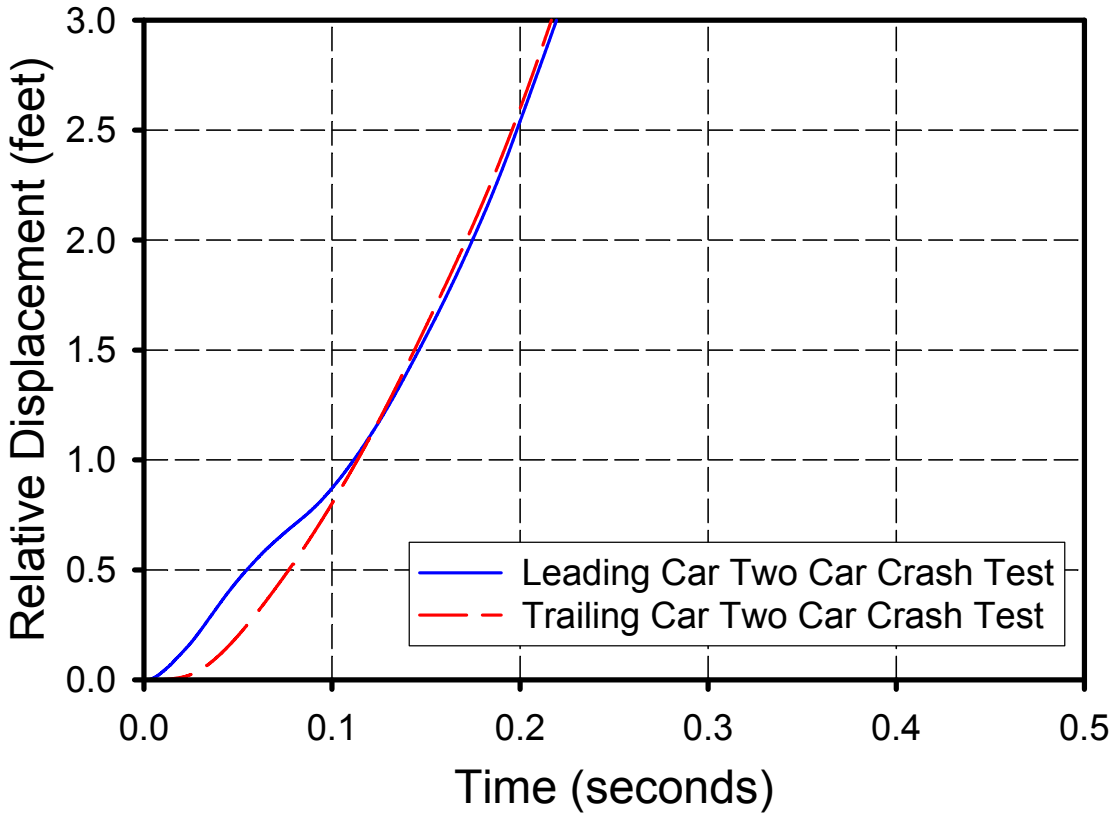


**Figure 25. Forward-Facing Unrestrained Occupant Longitudinal Relative Displacement/Time History**

Since the cars are pitching during the impact, the vertical displacements vary along the lengths of the cars. The maximum vertical upward displacement of the carbody after 0.20 seconds is approximately 2 inches (5 cm) near the lead body bolster and the maximum displacement downward is approximately 1 inch (2.5 cm) near the trailing body bolster. The upward displacement of the carbody results in the downward relative displacement of the occupant; at this location the point of contact of an unrestrained occupant's head would move down the seat back ahead, closer to the floor by several inches. Such motions are not likely to influence the likelihood of injury. At the rear body bolster, however, relative displacement is upward, and the occupant's head may miss or only partially impact the seat ahead. Such motions may significantly increase the head load, increasing the likelihood of injury.

Relative lateral motion greater than 1 foot (30 cm) is required for the head of the aisle-side occupant to miss the back of the seat ahead, and similar relative displacements are required for the wall-side occupant to strike the wall. Even though the lateral displacements vary along the length of the car, for the initial 0.20 seconds, these displacements remained significantly less than 1 foot. (The lateral motions of the cars did indeed exceed one foot some time after 0.20 seconds. It is assumed that, once the occupant contacts the interior, the longitudinal deceleration in combination with friction is sufficient to keep the occupant in contact with the interior. The lateral accelerations are nearly an order of magnitude less than the longitudinal accelerations.)

Figure 26 shows a plot of the longitudinal velocity of an unrestrained occupant relative to the interior of the car as a function of that occupant's longitudinal displacement relative to the interior of the car. The greater the relative velocity of the secondary impact, the greater the

likelihood of occupant injury. The plot shows the relative velocity for test dummies in the leading and trailing cars, the longitudinal velocity associated with the 8 G-triangular crash pulse used in previous sled testing, as well as the relative velocity measured in the single-car test conducted in November 1999. The 8-G triangular pulse results in a secondary-collision velocity that is approximately 30 percent greater than the pulses measured during the two-car test. The 8-G crash pulse is more likely to result in passenger injury than the crash pulses measured during the two-car test, for forward-facing unrestrained occupants.

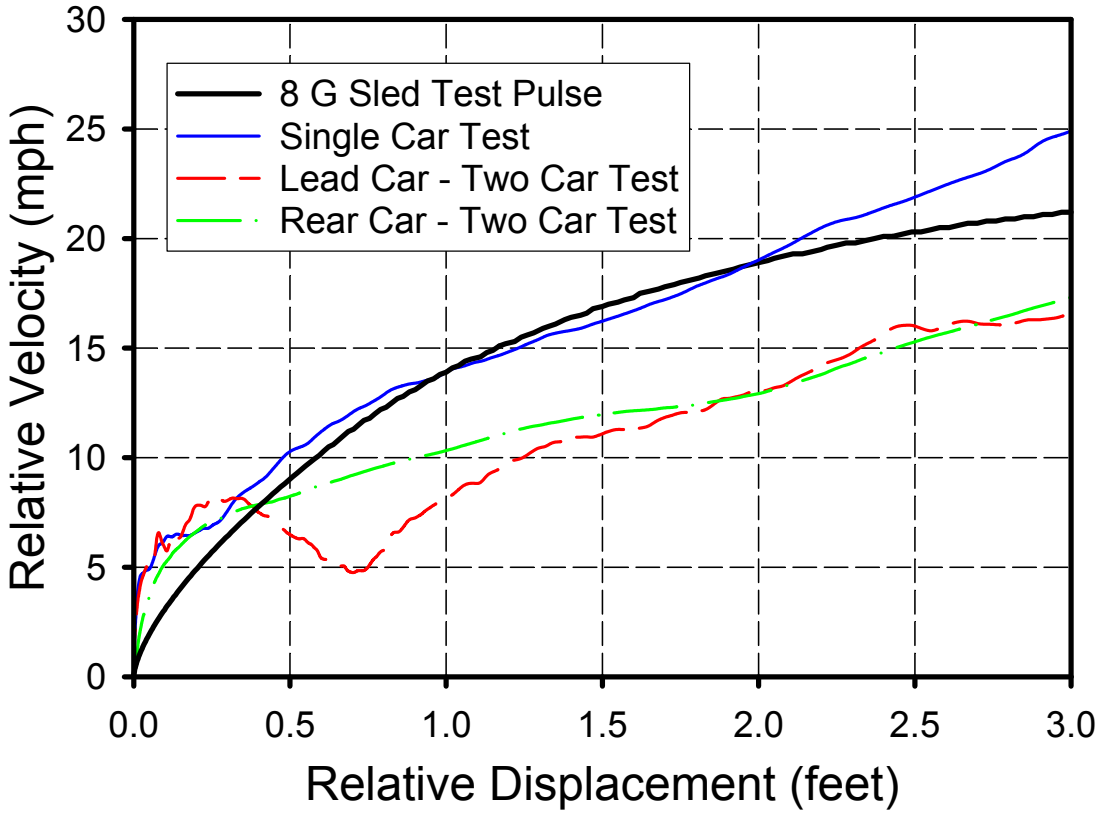


**Figure 26. Relative Longitudinal Velocity of an Unrestrained Occupant as a Function of Relative Longitudinal Displacement**

# 5. DISCUSSION AND CONCLUSIONS

As laid out in the test plans, the gross motion of the carbody was measured, as was the force/crush behavior at the impacting end of the car. The car-to-car interaction was observed along with the failure modes of the principal structural members. The effectiveness of the different occupant-protection strategies is covered in Reference 16.

The single-car and two-car collision-dynamics models have been modified to better agree with the results from both tests. The model estimates the gross motion and force/crush behavior from the respective tests reasonably well.

The results from the first two full-scale tests were used to characterize the collision behavior of conventional commuter-rail cars. The results indicate that the force/crush behavior is not influenced by the failure mode of the principle structural members. The model can be extrapolated to look at frontal collisions involving more coupled cars and at varying collision speeds. The model can also be modified to evaluate the influence of different force/crush characteristics on the secondary-impact velocity that an occupant would experience in a collision.

The results from the two-car test have been used to demonstrate that the trailing car serves to reduce the severity of the acceleration/time history of the leading car. The force applied to the leading car by the trailing car minimizes the duration of the initial acceleration peak of the leading car, which reduces the secondary-impact velocity when an occupant strikes the interior.

The collision-dynamics model predicted the lateral buckling of the cars when there was a small perturbation in the direction of the impact force. However, the model could be improved to better capture the timing of the longitudinal forces transferred through the coupler. From the test data, it appears that the coupler compresses several inches before any significant force develops. Tuning this "gap" in the model will result in a better estimation of the timing of the acceleration peaks of both cars. Also, the model requires more damping at the coupler to minimize the longitudinal oscillation of both cars. In future work, the coupler element will be refined to better estimate the timing in the development of the force at the coupler, and to minimize the longitudinal oscillation of the cars. The two-car collision-dynamics model will then be extended to model the train-to-train test scheduled for the fall of 2001.

Relative impact velocity can be used to compare the relative severity of different collisions with different crash pulses. Previous sled tests have been conducted using a triangular crash pulse, or acceleration/time history, with a peak of 8 Gs and a duration of 0.25 seconds. This acceleration/time history was developed from earlier single degree of freedom collision-dynamics models, in lieu of actual test data. The 8 G-acceleration curve may appear much less benign than the acceleration curves measured in the single-car and two-car tests because the peak of 8 Gs is much less than the 32-38 G-peak measured in the impacting car from the two tests. However, the corresponding secondary-impact velocities for test dummies subjected to the 8 G-crash pulse would be 19 mph (30.4 km/h) and 20 mph (32 km/h) for unrestrained, forward-facing dummies seated in commuter seats and intercity seats, respectively (see Appendix C). The corresponding secondary-impact velocities for the two-car test were significantly lower at 13 mph (20.8 km/h) and 15 mph (24 km/h), respectively. Therefore, the peak acceleration cannot be taken alone as a measure of collision severity. A more detailed comparison of the 8 G crash pulse with the measurements from the tests is planned following a full-scale test 3; the train-to-train impact test of conventional equipment.

# REFERENCES


1. Mayville, R.A., et al., "Locomotive Crashworthiness Research," Volumes 1 through 5, DOT/FRA/ORD-95/8.1-8.5, 1995.

2. Tyrell, D.C., et al., "Evaluation of Cab-car Crashworthiness Design Modifications," *Proceedings of the 1997 IEEE/ASME Joint Railroad Conference*, IEEE Catalog Number 97CH36047, 1997.

3. Tyrell, D.C., K.J. Severson, and B.P. Marquis, "Crashworthiness of Passenger Trains," U.S. Department of Transportation, DOT/FRA/ORD-97/10, 1998.

4. Mayville, R.A., R.J. Rancatore, L. Tegler, "Investigation and Simulation of Lateral Buckling in Trains," *Proceedings of the 1999 IEEE/ASME Joint Railroad Conference, April 13-15, 1999*, IEEE Catalog Number 99CH36340, ASME RTD Volume 16, 1999.

5. Tyrell, D.C., et al., "Locomotive Crashworthiness Design Modifications Study," *Proceedings of the 1999 IEEE/ASME Joint Railroad Conference, April 13-15, 1999*, IEEE Catalog Number 99CH36340, ASME RTD Volume 16, 1999.

6. Stringfellow, R.G., R.A. Mayville, R.J. Rancatore, "A Numerical Evaluation of Protection Strategies for Railroad Cab-car Crashworthiness," *Proceedings of the 8th ASME Symposium on Crashworthiness, Occupant Protection and Biomechanics in Transportation November 14-19, 1999*; Nashville, Tennessee, 1999.

7. Mayville, R.A., R.P. Hammond, K.N. Johnson, "Static and Dynamic Crush Testing and Analysis of a Rail Vehicle Corner Structural Element," *Proceedings of the 8th ASME Symposium on Crashworthiness, Occupant Protection and Biomechanics in Transportation November 14-19, 1999*; Nashville, Tennessee, 1999.

8. Holmes, B.S. and J.D. Colton, "Application of Scale Modeling Techniques to Crashworthiness Research," Kenneth J. Saczalski, et al. Editors, *Aircraft Crashworthiness*, Charlottesville, Virginia: University Press of Virginia, 1975.

9. Tyrell, D., K. Severson, A.B. Perlman, "Single Passenger Rail Car Impact Test Volume I: Overview and Selected Results," U.S. Department of Transportation, DOT/FRA/ORD-00/02.1, March 2000.

10. VanIngen-Dunn, C., "Single Passenger Rail Car Impact Test Volume II: Summary of Occupant Protection Program," U.S. Department of Transportation, DOT/FRA/ORD-00/02.2, March 2000.

11. Brickle, B., "Single Passenger Rail Car Impact Test Volume III: Test Procedures, Instrumentation, and Data," DOT/FRA/ORD-01/02.3, May 2000.

12. Severson, K., "Development of Collision Dynamics Models to Estimate the Results of Full-scale Rail Vehicle Impact Tests" Tufts University Master's Thesis, November 2000.

13. Tyrell, D., et al., "Rail Passenger Equipment Crashworthiness Testing Requirements and Implementation," presented at the 2000 International Mechanical Engineering Congress and Exposition, Orlando, Florida, November 6, 2000.

14. Severson, K., D.C. Tyrell, A.B. Perlman, "Rail Passenger Equipment Collision Tests: Analysis of Structural Measurements," presented at the 2000 International Mechanical Engineering Congress and Exposition, Orlando, Florida, November 6, 2000.

15. Tyrell, D., J. Zolock, C. VanIngen-Dunn, "Rail Passenger Collision Tests: Analysis of Occupant Protection Measurements," presented at the 2000 International Mechanical Engineering Congress and Exposition, Orlando, Florida, November 6, 2000.

16. VanIngen-Dunn, C., "Passenger Rail Two-Car Impact Test Volume II: Summary of Occupant Protection Program," U.S. Department of Transportation, DOT/FRA/ORD-01/22.II, January 2002.

17. Brickle, B., "Passenger Rail Two-Car Impact Test Volume III: Test Procedures, Instrumentation, and Data," DOT/FRA/ORD-01/22.III, January 2002.

18. National Transportation Safety Board, "Railroad Accident Report: Head-On Collision of Boston and Maine Corporation Extra 1731 East and Massachusetts Bay Transportation Authority Train No. 570 on Former Boston and Maine Corporation Tracks, Beverly, Massachusetts, August 11, 1981," PB82-916301, NTSB-RAR-82-1, 1982.

19. National Transportation Safety Board, "Collision and Derailment of Maryland Rail Commuter MARC Train 286 and National Railroad Passenger Corporation, AMTRAK Train 29 Near Silver Spring, Maryland on February 16, 1996," RAR-97-02, PB97-916302 , 1997.

20. National Transportation Safety Board**, "**Collision of Northern Indiana Commuter Transportation District Train 102 with a Tractor-Trailer Portage, Indiana June 18,1998," RAR-99-03, 07/26/1999.

21. National Transportation Safety Board**, "**Collision of Reading Company Commuter Train and Tractor-Semitrailer, Near Yardley Pennsylvania, June 5, 1975," RAR-76-4, 03/03/1976.

22. White, J.H., Jr., "The American Railroad Passenger Car," The Johns Hopkins University Press, 1978.

23. Kirkpatrick, S.W., and J.W. Simons, "High-Speed Rail Collision Safety," in *Rail Vehicle Crashworthiness Symposium*, DOT/FRA/ORD-97/08, 1998.

24. Tyrell, D.C., and K.J. Severson, "Crashworthiness Testing of Amtrak's Traditional Coach Seat," DOT/FRA/ORD-96/08, October 1996.

25. Woodbury, C.A., 3rd, "North American Passenger Equipment Crashworthiness: Past, Present, and Future," in *Rail Vehicle Crashworthiness Symposium*, DOT/FRA/ORD-97/08, 1998.

26. U.S. Department of Transportation, Federal Railroad Administration, "49 CFR Part 216, et al., Passenger Equipment Safety Standards; Final Rule," *Federal Register*, May 12, 1999.

27. American Public Transportation Association, *Manual of Standards and Recommended Practices for Rail Passenger Equipment*, July 1, 1999.

28. Hanefi, E.H., and T. Wierzbicki, "Calibration of Impact Rigs for Dynamic Crash Testing," Joint Research Center, European Commission Institute for Safety Technology, Report EUR 16347 EN, 1995.

29. U.S. Department of Transportation, National Highway Transportation Safety Administration, "49 CFR Part 552, 571, 585 and 595, RIN 2127-AG70 "Federal Motor Vehicle Safety Standards; Occupant Crash Protection," May 2000.

30. Association of American Railroads Technical Services Division, "Locomotive Crashworthiness Requirements, Standard S-580," *Mechanical Section - Manual of Standards and Recommended Practices*, Adopted: 1989, Revised, 1994.

31. ADAMS, Version 9.0.1, Mechanical Dynamics, Inc., Ann Arbor, Michigan.

# APPENDIX A. TEST REQUIREMENTS

Requirements for testing include the specification of the equipment to be tested, the conditions for the test, and the information to be gathered during the test. For the single-car test, requirements were developed from the results of car crush, train dynamics, and occupant response simulations. For the occupant-protection experiments, the requirements for previous sled testing were also considered [24]. The two-car test requirements were developed from simulations, as well as the experience gained in performing the single-car test. Similarly, the requirements for the train test are being developed from simulations of that test, as well as from the experience gained in the single-car and two-car tests.

## 1. PRE-TEST MODELING AND SIMULATION

The simulations have been used to bound the range of potential responses of the equipment and the dummies inside the cars. The results have been used for determining critical measurements, the sizing and the placement of instruments, and the location of dummies for the occupant-protection tests. A three-step approach is used to simulate the tests:

Step 1: Car Crush Behavior. Detailed dynamic, non-linear, large displacement finite-element models of the structures are developed. The principal purpose of these models is to calculate the force/crush behavior for use in the crush elements of the collision-dynamics models.

Step 2: Train Collision Dynamics. Plane and three-dimensional lumped-mass collision-dynamics models are developed and applied to determine the trajectories of the equipment. Impact elements are used in these collision-dynamics models, with the parameters for these elements taken from the results of the finite-element analyses of car crush behavior.

Step 3: Occupant Response. The occupant volume reduction and decelerations developed from the collision-dynamics models are used to determine the response of the occupants during a train collision, and the loads imparted to the seats and other interior fixtures.

## 2. SINGLE-CAR TEST

The equipment tested during the single-car test was a cab-car of conventional design built to North American standards. Figure A-1 shows a schematic illustration of the major structural elements of a conventional single-level passenger car. In a typical arrangement, the operator stands on a plate over one of the step wells, or sits on a chair that folds out from the vestibule wall.

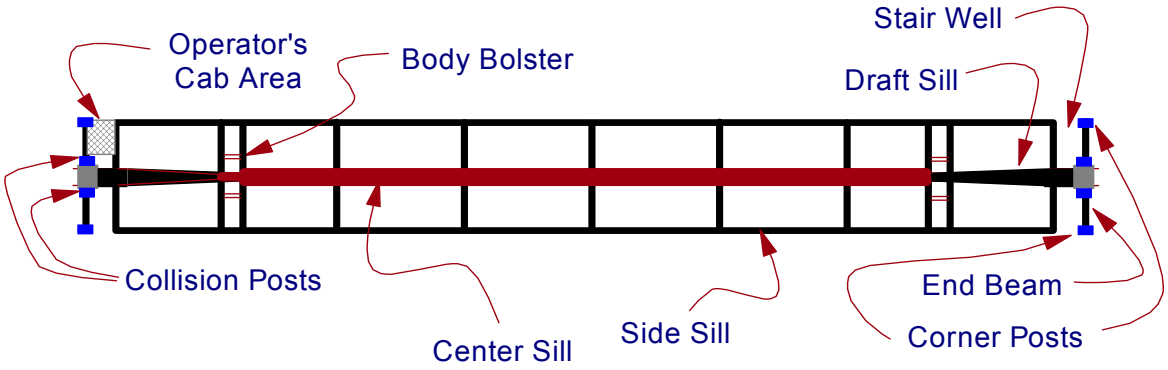


**Figure A-1. Schematic of Typical Cab-car Structural Members, Top View**

The North American standard that most influences the collapse of the car structure is the requirement for 800 kips buff strength. This standard requires that the complete car be able to support an 800 kip squeeze load applied to the buff stops, which are located on the draft sill approximately 4 feet (1.2 m) in from the end of the car, without permanent deformation. This requirement has been in effect since 1939 [25] and continues to be in effect [26, 27]. Most of the recent changes to North American practice for passenger equipment used at speeds less than 125 mph (200 km/h) have been to the end structure of the car, i.e., the collision post and corner post requirements. These elements do not influence the longitudinal strength of the car. The buff strength requirement does influence the longitudinal strength of the car.

The test conditions are intended to produce substantial damage to the car structure. At least three feet of crush was desired in order to measure the data necessary to evaluate the effectiveness of models in predicting large amounts of structural damage. The simulation results indicated an impact speed of 35 mph (56 km/h), with a fixed barrier being necessary to produce 3 to 5 feet of crush (reduction in length) of the carbody.

## 2.1 Required Information

For the single-car test, the information desired on structural crashworthiness included:

- the force imparted to the wall during the test,
- the relative loadings carried by the longitudinal structural members,
- the mode of crush of the carbody (i.e., the series of geometric changes the car structure undergoes as it crushes),
- the elastic vibratory motions of the carbody,
- the gross motions of the car, including the longitudinal, vertical and lateral accelerations and displacements,
- the gross motions of the trucks, including the longitudinal, vertical and lateral accelerations and displacements, and
- the displacements across the suspension elements.

The force/crush characteristic (i.e., the load that the car structure develops as it collapses) is a key characteristic of the crashworthiness of a car. Analytically, this information is often calculated with detailed finite-element models that incorporate the geometry of the structure and the properties of the material. This information is then used in models of the entire train to determine the distribution of crush among the cars of the train and the decelerations of each of

the cars. If the force/crush characteristic is incorrect, then the results of the train model will also be incorrect. One purpose of the test is to make measurements for comparison with analytic predictions in order to assure that such predictions are accurate.

The mode of crush is particularly difficult to calculate for strength-design structures, such as conventional North American design rail-passenger cars. The mode is sensitive to small imperfections in the structures [28]. Because of the sensitivity to small imperfections, precise agreement between the mode predicted by analysis and that observed during the test is not likely.

The vertical and lateral motions of the car are of particular interest in the test. Any vertical or lateral forces that develop as the car crushes can elicit a response from the suspension. Analysis results indicate that small lateral or vertical forces, relative to the longitudinal force, are required in order to cause significant vertical and lateral carbody motions. Such forces may come about because the structure effectively forms a ramp as it crushes. It is likely that the combination of the vertical forces and suspension response influence the potential for override.

The desired information on occupant protection for each of the interior configurations includes:

- the potential for occupant injury,
- the kinematics of the occupants, and
- loads imparted to the seats.

There are currently criteria for head, neck, chest, and femur injury used in the automotive industry [29]. These criteria relate acceleration and force measurements to the potential for human injury. It was desired to make the measurements required for comparison with the criteria for the three interior configurations. These measurements would also be useful for comparison with previous analyses predictions and sled test measurements.

It was particularly desired to gather information on the influence of the vertical and lateral motions of the car on the occupant kinematics. Previous analyses and sled testing have been one-dimensional; the vertical and lateral accelerations have been neglected. The information gathered during the test will be used to evaluate the assumption that the longitudinal deceleration dominates to such a degree that the lateral and vertical motion can be neglected in evaluating occupant-protection strategies.

In order to be effective in providing compartmentalization for unrestrained occupants, the seats and interior fixtures must remain attached during a collision. It was desired to measure the loads imparted to the seats. Such information can be used for comparison with simulation analyses, as well as in development of future seat designs.

## 3. TWO-CAR TEST

Requirements for the equipment tested in the two-car test were the same as in the single-car test; the equipment was built to North American standards. The only difference being that two coupled cars impacted the fixed barrier in the two-car test.

Like the single-car test, it was desired that the test conditions produce substantial damage to the car structure, i.e., 3 to 5 feet (.91 to 1.5 m) of crush. The simulation results indicated an impact speed of 26 mph, with a fixed barrier being necessary in order to produce 3 to 5 feet of crush

(reduction in length) of the leading carbody. The simulation results also indicated that essentially all of the crush would be focused at the leading end of the leading car with very little crush at the trailing end of the leading car, or at the leading end of the trailing car.

### 3.1 Required Information

The required information for the two-car test was the same as for the single-car test, with the addition of information on the interactions of the coupled cars.

Simulations made prior to the test indicated that the coupled cars would sawtooth buckle, as illustrated in Figure A-2. Schematic (a) shows the coupler in its nominal position, schematic (b) shows the coupler when it has buckled, and schematic (c) shows the cars when a sawtooth buckle has occurred. It was desired to gather information on the forces acting on the coupler and the timing of the buckle; i.e., when the buckle occurred in relation to the crush of the leading car. This information is required for comparison with simulation predictions to assure that the coupler and its behavior is being appropriately modeled.

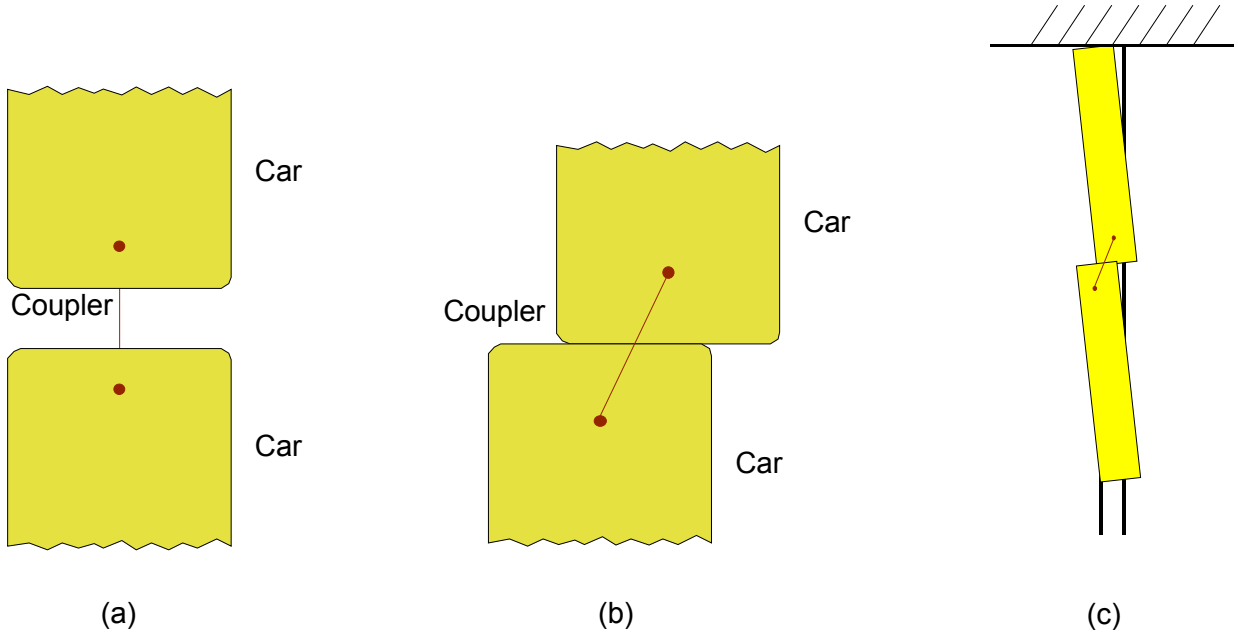


**Figure A-2. Schematics of Sawtooth Lateral Buckling (adapted from reference [4])**

The desired information on the interactions of the coupled cars includes:

- longitudinal force acting on the couplers,
- the longitudinal, lateral, and vertical displacements of the couplers relative to the respective carbodies, and
- the longitudinal, lateral, and vertical displacements of the cars relative to each other.

## 4. TRAIN TEST

The equipment requirements for the train test are the same as for the single-car and two-car tests; the equipment was built to North American standards. In addition to cab and coach cars, this test also requires a locomotive. The requirement for the locomotive is that it comply with AAR

standard S-580 [30]. Since there is a potential for either the locomotive overriding the cab-car or vice versa, the cab-car end structure (collision posts and corner posts) must also comply with current APTA standards [26] and FRA regulations [27].

The details of the test conditions for the train test are currently being finalized. It is desired to cause substantial damage to the leading cab-car and to the coach immediately trailing behind it.

## 4.1 Required Information

In addition to the information gathered during the single-car and two-car tests, it is also desired to gather information on the interactions between the colliding vehicles. There is a potential for override to occur during the test. Override occurs owing to the combined effects of the initial geometry of the vehicles (e.g., sill heights), crush of the vehicle structures, and the responses of the vehicles on their suspensions. Information on each of these factors is required to assure that each of these factors is appropriately taken into account in simulation models.

The desired information on the interactions of the colliding locomotive and cab-car includes:

- longitudinal, vertical, and lateral forces at the colliding interface, and
- the longitudinal, lateral, and vertical displacements of the colliding locomotive and car relative to each other.

# APPENDIX B. PARAMETERS USED IN TWO-CAR COLLISIONS-DYNAMICS MODEL

The collision-dynamics model was developed using the ADAMS computer program [31]. Contact between the rigid impact wall and the front plate of the colliding vehicle is governed by an impact element. This impact element generates an elastic restoring force based on Hertz contact when the colliding objects try to penetrate one another. The impact stiffness and damping values are 6.0E+07 lb/ft and 2.0E+04 lb-s/ft, respectively. These parameters were chosen heuristically, to help represent the dynamic portion of the impact force [12].

The front end plate is connected to the main carbody by five springs. The springs account for the dominant structural elements: draft sill, side sills, and roof plates. The majority of the longitudinal load is born by the draft sill. The corresponding force/crush curves are plotted in Figure B-1. These force/crush curves were derived from the test data [12].

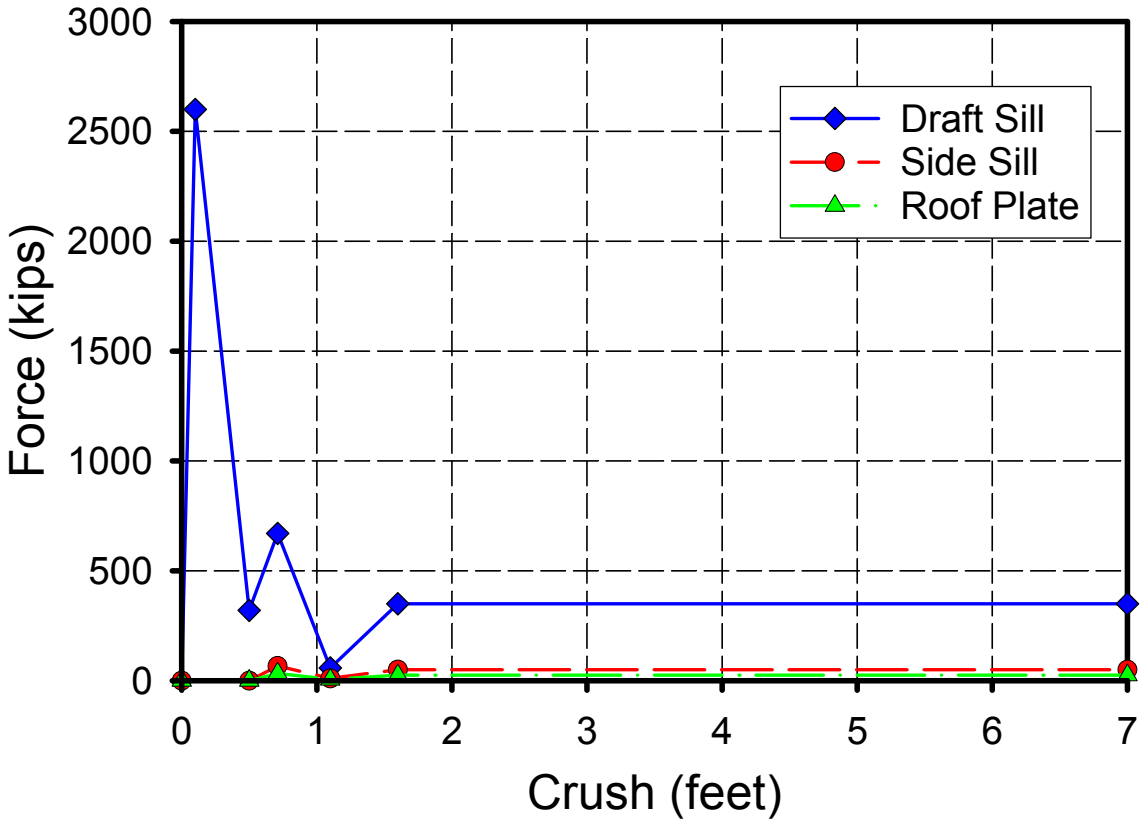


**Figure B-1. Longitudinal Force/Crush Behavior of Collision Springs**

The secondary suspension between the trucks and car bodies is a combination of spring and damper elements that are linear for small displacements and represent compression and extension stops for large displacements. These elements transmit forces between the car bodies and trucks in the lateral, longitudinal, and vertical directions. Each truck has elements to transmit vertical and lateral forces to the rails, one for each rail.

Both kinematic and flexibility characteristics are accounted for in the coupler connection between the two vehicles.

Table B-1 lists the centroidal mass and principal mass moments of inertia that were prescribed to represent the bodies of the leading passenger car in the two-car model. These values were adapted from a similar ADAMS trainset model [4].

**Table B-1. Vehicle Parameters**

| Property | Main Body | Trucks | Front Plate |
|---|---|---|---|
| Mass (lb-m) | 35,579 | 13,700 | 2,252 |
| Centroidal Roll (lbm-ft$^2$) | 9.67E+05 | 3.55E+04 | 9.617E+04 |
| Centroidal pitch (lbm-ft$^2$) | 2.22E+07 | 1.08E+05 | 4.746E+07 |
| Centroidal yaw (lbm-ft$^2$) | 2.24E+07 | 9.28E+04 | 4.894E+04 |

# APPENDIX C. SELECTED SINGLE-CAR TEST RESULTS

Both the test and analysis data [9] from the single-car test were reprocessed in accordance with J211.1. Accelerometer C-3 at the center of the car was used here, rather than C-2, which was used for data presented in [9]. Figure C-1 presents the force/crush behavior from the test results, collision-dynamics analysis and FE analysis. A comparison of the results in Figure C-1 with Figure 11 in [9] shows higher peak values for the reprocessed data, but there is little change in the steady force values.

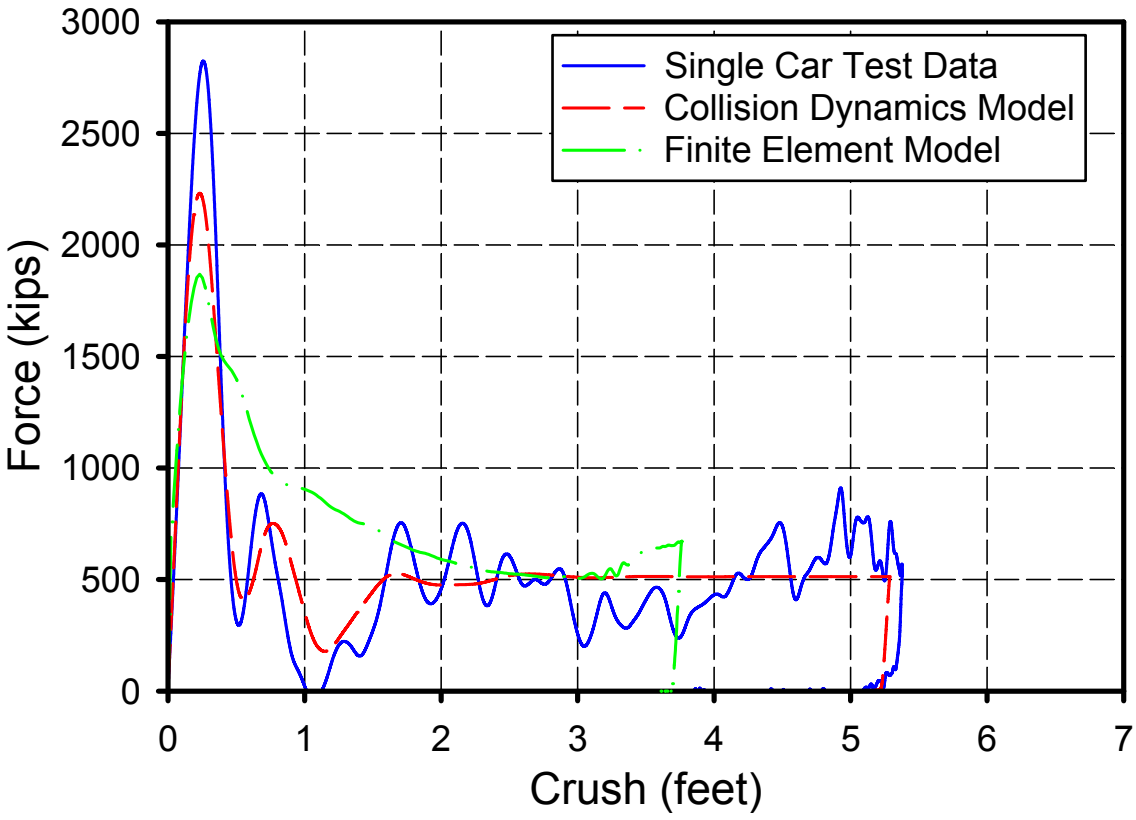


**Figure C-1. Comparison of Force/Crush Behavior**

Figure C-2 shows the reprocessed acceleration data. A comparison of the results in Figure C-2 with Figure 11 in Reference 9 shows the higher peak values for the reprocessed data, but there is little change in the steady acceleration values.

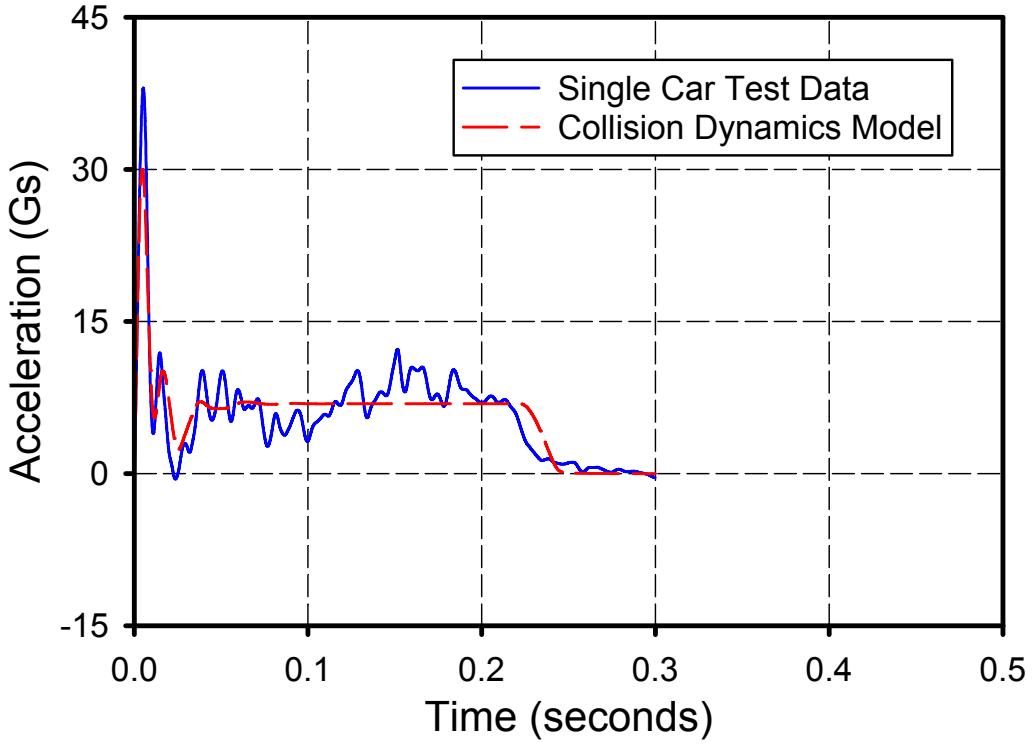


**Figure C-2. Comparison of Longitudinal Accelerations of Carbody CG**

Reprocessed data in Figure C-3 can be compared with the results in Figure 15 of Reference 9. In this case, the reprocessing of the data does not affect the results.

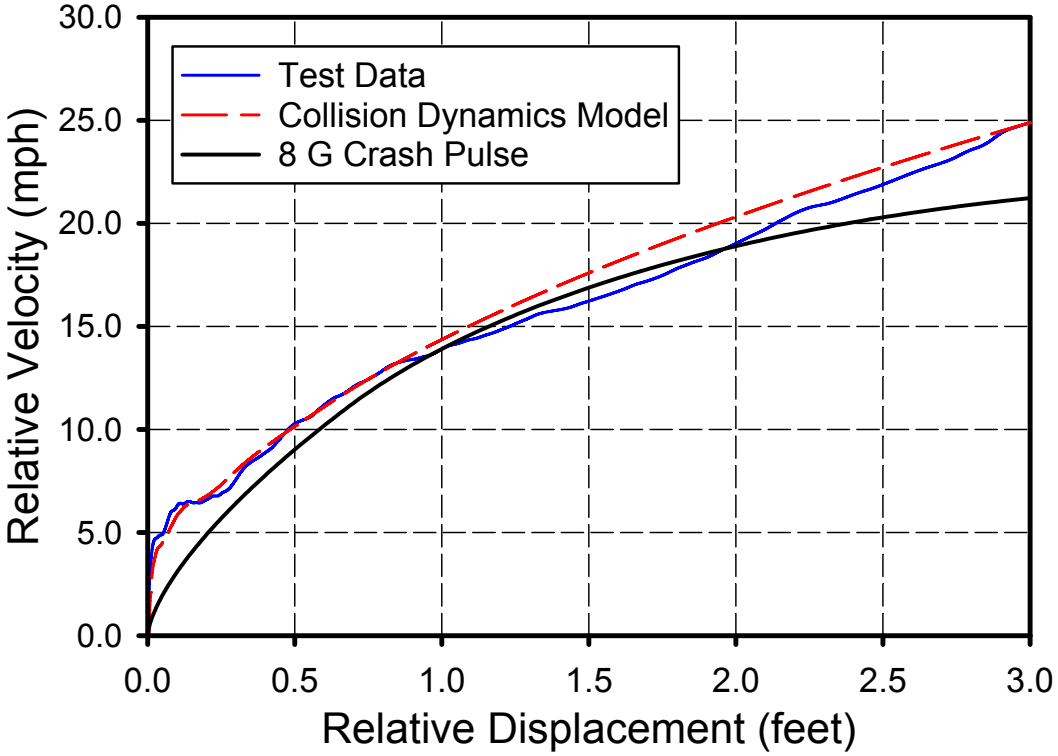


**Figure C-3. Comparison of Secondary-Impact Velocity for Dummies in Single-Car Test and an 8 G Sled Test**